Reviewed Preprint
v1 • November 18, 2025
Not revised

For correspondence:
davismj@health.missouri.edu

Competing interests: No competing interests declared

Funding: See page 32

Reviewing editor: Mohamed Trebak, University of Pittsburgh, United States of America

Roles of G-protein coupled receptors and mechanosensitive ion channels in pressure-induced chronotropy of lymphatic vessels

Michael J Davis[1], Hae Jin Kim[1], Min Li[1], Jorge A Castorena-Gonzalez[2], Soumiya Pal[1], Timothy L Domeier[1], Joshua P Scallan[3], Scott Earley[4], Scott D Zawieja[1]

[1]Department of Medical Pharmacology & Physiology, University of Missouri, Columbia, United States • [2]Department of Pharmacology, Tulane University School of Medicine, New Orleans, United States • [3]Department of Molecular Pharmacology & Physiology, University of South Florida, Morisani School of Medicine, Tampa, United States • [4]Department of Pharmacology and Physiology, University of Rochester Medical Center, Rochester, United States

eLife Assessment

Davis and colleagues describe findings that are **fundamental** to the understanding of pressure mechanosensation in lymphatic vessels and are of significant importance to other areas of mechanosensory physiology. Based on many different knockout mouse models and rigorous state-of-the-art pressure myography recordings, they present **compelling** evidence that mechano-activation of GNAQ/GNA11-coupled GPCRs generates IP3, which induces Ca2+ release from internal stores through IP3R1 and drives depolarization through the activation of ANO1 Cl- channels to induce lymphatic vessel contractility. Nevertheless, some aspects of the manuscript are **incomplete**. The specific identity of the GPCR(s) involved remains to be uncovered, as evidence of frequency-pressure impairment is only demonstrated with abolition of GNAQ/GNA11action, not the receptors per se.

https://doi.org/10.7554/eLife.109466.1.sa3

Abstract

Active lymph pumping relies on the spontaneous contractions of collecting lymphatic vessels, with frequencies that are exquisitely sensitive to changes in intraluminal pressure. This homeostatic and mechanosensitive mechanism, termed pressure-induced lymphatic chronotropy, enables lymph transport to be matched to the filling state of the lymphatic capillaries. We investigated the mechanistic basis of pressure-induced chronotropy using ex vivo contraction assays of mouse popliteal collecting vessels, in which contraction frequency increased >10-fold with a 5 cmH_2O pressure change. The contractile, electrophysiological and transcriptional similarities between lymphatic muscle and arterial smooth muscle led us to hypothesize that pressure-dependent chronotropy shares a parallel signaling process to pressure-induce arterial depolarization/constriction. Thus, we investigated two major mechanisms: 1) pressure-induced activation of mechanosensitive cation channels, including TRPC6, TRPM4, PKD1/2, TRPV2 and ENaC, and 2) mechano-activation of GNAQ/GNA11-coupled GPCRs that would generate second messengers to activate those channels. We combined contraction assays with scRNAseq analysis of the respective targets and made maximum use of transgenic mice to avoid non-specific effects of pharmacological inhibitors, particularly those used to block TRP channels. Our findings rule out significant roles for TRP and other mechanosensitive channels implicated in myogenic constriction, as well as channels implicated in ionic pacemaking of other tissues, and instead

support a scheme whereby mechano-activation of GNAQ/GNA11-coupled GPCRs generates IP_3, which induces SR Ca^{2+} release through IP_3R1 and drives depolarization through the activation of ANO1 Cl^- channels.

Introduction

The lymphatic system is critically important for the maintenance of interstitial fluid balance. Because the Starling forces governing fluid movement across blood capillaries favor net filtration in most tissues (Levick & Michel, 2010), filtered fluid and protein will accumulate in the interstitium unless it is removed by the lymphatic system. Lymphatic capillaries are optimized to reabsorb that fluid, which can exceed 8 $L{\cdot}day^{-1}$ (Renkin, 1986). Once reabsorbed, lymph is transported by a combination of passive and active transport mechanisms through the collecting lymphatic vessel network, first to lymph nodes and eventually back into the venous system. Active lymph pumping relies on the spontaneous contractions of collecting lymphatic vessels—events that are initiated by action potentials (APs) in lymphatic muscle cells (LMCs). These contractions are relatively large in amplitude, with ejection fractions often exceeding 80% and sufficient to propel lymph through a system of one-way valves that ensure its unidirectional movement (Davis *et al*., 2025). Active pumping accounts for the majority of lymphatic transport in the lower legs of humans during quiet standing (Olszewski & Engeset, 1980) and facilitates lymph return against adverse hydrostatic pressure gradients that develop under gravitational loads (Davis *et al*., 2012; Scallan *et al*., 2016; Li *et al*., 2022). An important feature of the active lymph pump system is the exquisite sensitivity of the spontaneous contraction frequency of collecting lymphatic vessels to changes in their intraluminal pressure, enabling lymph transport to be matched to the filling state of the lymphatic capillary network (Scallan *et al*., 2012). This homeostatic mechanism is termed “pressure-induced lymphatic chronotropy” (Zawieja *et al*., 2019). In popliteal collecting vessels of the mouse hindlimb, the spontaneous contraction frequency can increase from 2 to 20 $contractions{\cdot}min^{-1}$ as pressure is elevated from 0.5 to 10 cmH_2O, i.e., a 10-fold increase over the physiological pressure range of those vessels (Davis *et al*., 2020; Davis *et al*., 2023a; Davis *et al*., 2023b). Contraction amplitude increases modestly over a portion of the same pressure range (Scallan *et al*., 2012), but modulation of contraction frequency is the primary determinant of active lymph transport.

Pressure-induced chronotropy reflects an underlying mechanotransduction process that ultimately involves control of an intrinsic pacemaker in LMCs by intraluminal pressure. Although the specific force sensing mechanism is unknown, contractile, electrophysiological and transcriptional similarities between LMCs and vascular smooth muscle cells (VSMCs) support the hypothesis that pressure-dependent chronotropy shares a parallel signaling process to the myogenic response of VSMCs. The myogenic response refers to in rapid increase in arterial pressure induces distention of a small artery / arteriole, which then constricts over time until a new, stable diameter lower than the original diameter is reached (Davis, 2012). A similar constriction often occurs in collecting lymphatic vessels simultaneously with pressure-induced chronotropy (Davis *et al*., 2009). Pressure-induced arterial constriction is preceded by VSM depolarization (Harder, 1984) and several lines of evidence support a critical role for the activation of (putative) mechanosensitive cation channels in that process—in particular the involvement of three TRP channel family members: TRPC6, TRPM4 and PKD1/2.

The first evidence for a molecularly identified ion channel involved in myogenic constriction came from the demonstration that single channel currents in VSMCs isolated from rat cerebral arteries were activated by patch pipette suction and those currents, along with pressure-induced cerebral artery constrictions and depolarizations, were attenuated after downregulation of TRPC6with antisense oligonucleotides (Welsh *et al*., 2002). TRPM4 channels were likewise implicated after inward, TRPM4-like currents in rat pial artery myocytes were found to be activated by membrane stretch, and because antisense- or siRNA-mediated knock down of TRPM4 significantly attenuated pressure-induced depolarization and myogenic tone development in those arteries (Earley *et al*., 2004b; Gonzales *et al*., 2014). However, results from *Trpc6*$^{-/-}$ and *Trpm4*$^{-/-}$ mice tended to contradict the above studies in finding no differences or even *enhanced*

arterial myogenic constriction in the global knock out animals (Dietrich *et al*., 2005; Mathar *et al*., 2010; Schleifenbaum *et al*., 2014). Evidence also supports roles for PKD2 (previously described as TRPP1) channels in myogenic constriction, but it, too, is controversial. Jaggar and colleagues reported that shRNA-mediated down-regulation of *Pkd2*attenuated pressure-induced depolarization and myogenic tone in rat pial arteries (Narayanan *et al*., 2013) and that pressure-induced constriction was blunted in hindlimb arteries isolated from Myh11-CreER^{T2};*Pkd2$^{f/f}$* (smooth muscle knockout, smKO) mice (Bulley *et al*., 2018). However, a study by Honoré and coworkers suggested that stretch-activated cation currents and myogenic constriction in mouse mesenteric artery smooth muscle were mediated by PKD1 channels (previously termed TRPP2), and that PKD2 channels played a counteracting role (Sharif-Naeini *et al*., 2009). Myogenic responses could not be tested in global *Pkd2* KO mice because constitutive deletion of *Pkd2* is embryonically lethal (Wu *et al*., 1998).

More recent work points to G-protein-coupled receptors (GPCRs) rather than TRP or other ion channels as the primary mechanosensing elements in the arterial myogenic response. Studies of cardiomyocytes first demonstrated that the angiotensin receptor, AT_1R, a GNAQ/GNA11-coupled GPCR, could be activated by mechanical stress through a mechanism independent of its ligand (Zou *et al*., 2004). Gudermann and coworkers provided compelling support for this mechanism using patch-clamped HEK293 cells, co-expressing AT_1R and TRPC6 channels, with hypoosmotic swelling as a mechanical stimulus (Mederos y Schnitzler *et al*., 2008). Two critical findings were 1) that TRPC6 current was activated by hypoosmotic swelling *only* if the cells co-expressed *Agtr1* (Mederos y Schnitzler *et al*., 2008) and 2) that the swelling-induced currents were largely prevented by inverse AT_1R agonists. *Agtr1* could be replaced by another GNAQ/GNA11-coupled GPCR, or *Trpc6* by another DAG-sensitive TRP channel (Mederos y Schnitzler *et al*., 2008). Subsequent studies from multiple laboratories, using selective pharmacological inhibitors of AT_1R, acute *Agtr1* knockdown, and/or mice deficient in *Agtr1* or other GNAQ/GNA11-coupled GPCRs, confirmed that basic principle in VSMCs: that pressure-induced constriction of many different types of arteries is transduced primarily, or exclusively, by GNAQ/GNA11-coupled GPCRs (Blodow *et al*., 2014; Harraz *et al*., 2014; Li *et al*., 2014b; Schleifenbaum *et al*., 2014; Pires *et al*., 2017; Bjorling *et al*., 2018). Helix 8 in the GPCR c-terminus was subsequently identified as the essential structural motif endowing mechanosensitivity (Erdogmus *et al*., 2019). The collective data support a model in which phospholipase C is activated downstream from GNAQ/GNA11-coupled GPCRs in response to elevated pressure, leading to increased production of DAG and IP_3/Ca^{2+} release, which activate TRPC6 and TRPM4 channels, respectively, to depolarize the cell and increase the open probability of L-type voltage-gated Ca^{2+} channels, thereby promoting global Ca^{2+} influx and contraction (Davis *et al*., 2023c). In a similar manner, TRPM4 and PKD2/2 channels might be activated by Ca^{2+} influx/release downstream from mechano-activation of a GPCR or another Ca^{2+}-permeable ion channel such as PIEZO1 (Peyronnet *et al*., 2013) or TRPV4 (Swain & Liddle, 2021).

Whether a similar scheme is operative in LMCs is unknown. Each lymphatic contraction is preceded by a near-linear depolarization from the “resting” potential to threshold potential, termed the diastolic depolarization, which is the primary determinant of AP/contraction frequency (Zawieja *et al*., 2025). Thus, lymphatic pressure elevation manifests not as a stepwise increase in baseline potential LMCs (von der Weid *et al*., 2014; Davis & Zawieja, 2018) but rather as an increase in the diastolic depolarization slope and a reduction in time required to reach threshold for AP firing (Zawieja *et al*., 2018b; Zawieja *et al*., 2019). Previously, we found that regulation of the diastolic depolarization slope was mediated largely by activation of the Ca^{2+} activated chloride channel ANOCTAMIN 1 (ANO1, also referred to as TMEM16A). ANO1 is not intrinsically mechanosensitive, but is regulated by Ca^{2+} and, in LMCs specifically, by IP_3 receptor 1-mediated Ca^{2+} release from sarcoplasmic reticulum (Zawieja *et al*., 2019; Zawieja *et al*., 2023), possibly downstream from one or more mechanosensitive GPCRs. However, other mechanisms are also involved because *Ano1* deletion from smooth muscle or pharmacological inhibition of ANO1 does not completely eliminate spontaneous APs or contractions (Zawieja *et al*., 2019). The primary goal of the present study was to test the roles of putative VSMC mechanosensitive ion channels, channels implicated in the regulation of pacemaking in other cell

types, and GNAQ/GNA11-coupled GPCRs in pressure-induced chronotropy of popliteal lymphatic vessels. An advantage in studying this particular aspect of lymphatic vessel mechanotransduction is the high sensitivity of the spontaneous contraction frequency to pressure, increasing ~10-fold over only a 5 cmH_2O pressure range in popliteal lymphatics compared to relatively modest levels of myogenic constriction (50% change) over a 60 mmHg pressure range, even in the most myogenically reactive arteries (Davis *et al*., 2023c). As part of our strategy, we sought to make maximum use of transgenic mice to avoid non-specific effects of pharmacological inhibitors, particularly those used to block TRP channels.

Materials and Methods

Protocol approval

All procedures were reviewed and approved by the animal care committee at the University of Missouri and complied with the standards stated in the "Guide for the Care and Use of Laboratory Animals" (National Institutes of Health, revised 2011).

Mice

WT mice [C57Bl/6 (#000664) and SVF129 (#101043) strains], *Slc8a1*$^{-/-}$ (#025943) mice and *AT*$_{1a}$*R*$^{-/-}$ (#002682) mice were purchased from The Jackson Laboratory (Bar Harbor, Maine). Myh11-CreER^{T2}mice were gifts from Stefan Offermans (Max Plank Institute, GDR). Sperm from *Gna*$_{12}$$^{-/-}$*;Gna*$_{13}$$^{f/f}$ and *Gna*$_{11}$$^{-/-}$*;Gna*$_q$$^{f/f}$ mice were gifts from Stefan Offermanns, after which the respective mice were rederived at MMRC, Columbia, MO to generate Myh11-CreER^{T2}*;Gna*$_{13}$$^{f/f}$*;Gna*$_{12}$$^{-/-}$mice *and* Myh11-CreER^{T2}*;Gna*$_q$$^{f/f}$*;Gna*$_{11}$$^{-/-}$mice. *Trpc6*$^{-/-}$ and *Trpc3*$^{-/-}$ mice were gifts from Lutz Birnbaumer (NIH); *Trpc6*$^{-/-}$ *;Trpc3*$^{-/-}$ double KO mice were generated by crossing those two strains. Myh11-CreER^{T2}*;Kcnq4*$^{f/f}$ *(encoding Kv7.4)* mice were a gift of Thomas Jentsch (Free Univ. of Berlin, GDR). *Piezo1*$^{f/f}$ mice were a gift from Ardem Pataputian (UCSD) and were bred to Myh11-CreER^{T2} mice to generate Myh11-CreER^{T2}*; Piezo1*$^{f/f}$ mice. *Ano1*$^{f/f}$mice, generated in the lab of Jonathan Jaggar (Leo *et al*., 2021) were bred to Myh11-CreER^{T2} mice to obtain Myh11-CreER^{T2}*;Ano1*$^{f/f}$ mice. *Itpr1*$^{f/f}$ mice were obtained from Ju Chen (UCSD) and bred to Myh11-CreER^{T2}mice to generate Myh11-CreER^{T2}*;Itpr1*$^{f/f}$mice. *Pkd2*$^{f/f}$ mice were generated in the University of Maryland PKD Core by Jonathan Jaggar, as previously described (Bulley *et al*., 2018), and bred in the Jaggar laboratory to Myh11-CreER^{T2}mice to generate Myh11-CreER^{T2}*;Pkd2*$^{f/f}$ mice. *Trpm4*$^{f/f}$mice were generated in the laboratory of Scott Earley and bred to Myh11-CreER^{T2} mice to produce Myh11-CreER^{T2}*;Trpm4*$^{f/f}$mice. *Trpv4*$^{f/f}$ mice were generated in the laboratory of Timothy Domeier (University of Missouri) and bred to Myh11-CreER^{T2} mice to produce Myh11-CreER^{T2}*;Trpv4*$^{f/f}$ mice. *Rosa26mTmG*$^{f/f}$ mice were purchased from JAX (#007676) and bred to Myh11-CreER^{T2} and Myh11-CreER^{T2}*;Ano1*$^{f/f}$ mice to produce Myh11-CreER^{T2}*;Rosa26mTmG*$^{f/f}$ *and* Myh11-CreER^{T2}*;Ano1*$^{f/f}$*; Rosa26mTmG*$^{f/f}$mice.

For genotyping, genomic DNA was extracted from tail clips using the HotSHOT method. Genotypes were determined by PCR with 2x PCR Super Master Polymerase Mix (Catalog # B46019, Bimake, Houston, TX) according to the provider's instructions. Mice containing Myh11-CreER^{T2} were induced with five consecutive daily injections of 100 mg tamoxifen (10mg/kg i.p.; in safflower oil). Those mice were studied a minimum of 2 weeks after induction. All floxed control mice were subjected to the same induction protocol. Because the Myh11-CreER^{T2} used for SM-specific deletion of floxed genes is carried on the y chromosome, only male mice were used for experiments involving Myh11-CreER^{T2} mice or their floxed controls. For other strains, both male and female animals were used.

Vessel isolation, pressure myography, and data acquisition

Mice were anesthetized with ketamine/xylazine (100/10 mg/kg, i.p.) and placed face down on a heated tissue dissection/isolation pad. The saphenous vein was exposed by a proximal-to-distal incision along the skin of the calf and the popliteal afferent lymphatic vessels on each side of the vein were isolated as previously described (Scallan & Davis, 2013). Each vessel was then pinned

with short segments of 40 μm stainless steel wire onto the SYLGARD-coated surface of a dissection chamber filled with BSA-supplemented Krebs buffer at room temperature. Once secured, the surrounding adipose and connective tissue were removed by microdissection. An isolated popliteal lymphatic vessel was then transferred to a 3-mL observation chamber, cannulated, pressurized to 3 cmH_2O using two glass micropipettes (50-60 μm outside diameter) and moved to the stage of a Zeiss inverted microscope. Lymphatic segments used in these studies typically contained a single valve. Polyethylene tubing attached to the back of each glass micropipette was connected to a two-channel computerized pressure controller (Scallan *et al*., 2013). To minimize diameter-tracking artifacts associated with longitudinal bowing at higher intraluminal pressures, input and output pressures were briefly set to 10 cmH_2O at the beginning of every experiment, and the vessel segment was stretched axially to remove longitudinal slack. The lymphatic vessel was then allowed to equilibrate at 37°C with inflow and outflow pressures set to 3 cmH_2O. Constant exchange of Krebs buffer was maintained using a peristaltic pump at a rate of 0.5 mL/min. After temperature stabilized, popliteal lymphatics typically began to exhibit spontaneous contractions within 10-15 min and stabilized in a consistent contraction pattern within ~30 minutes. Custom LabVIEW programs (National Instruments; Austin, TX) acquired real-time analog data and digital video through an A-D interface (USB-6216, National Instruments) and detected the inner diameter of the vessel at 30 fps using a Basler A641fm firewire camera (Davis, 2005). Videos of the contractile activity of lymphatic vessels were recorded for further analysis, if needed.

Assessment of ex vivo contractile function

The contractile parameters of each vessel were characterized at different levels of intraluminal pressure spanning the physiological range from 0.5 to 10 cmH_2O (in successive steps as follows: 3, 2, 1, 0.5, 3, 5, 8, and 10 cmH_2O). Spontaneous contractions were recorded at each pressure in typical intervals of 2 minutes, although a period of 4-5 min was sometimes required at the lowest pressure to obtain multiple contractions. During the pressure response protocol, both the input and output pressures were maintained at equal levels so that there was no imposed pressure gradient for forward flow. At the end of every experiment, all vessels were equilibrated by perfusion with calcium-free Krebs buffer containing 3 mM EGTA for 30 minutes, after which passive diameters were obtained at each level of intraluminal pressure.

Contractile function parameters

Once an experiment was completed, internal diameter traces and/or 30-fps brightfield videos of spontaneous contractions were analyzed using custom-written LabVIEW programs (Davis, 2023b, a) to detect end diastolic diameter (EDD), end systolic diameter (ESD), and contraction frequency (FREQ, computed on a contraction-by-contraction basis), with each parameter averaged over a 2-5 min period. These data were used to calculate the following commonly reported parameters that characterize the contractile function of lymphatic vessels:

$$\text{Amplitude} = \text{EDD-ESD} \quad (1)$$

$$\text{Normalized Contraction Amplitude} = \left(\frac{\text{EDD-ESD}}{D_{MAX}}\right) \times 100 \quad (2)$$

$$\text{Ejection Fraction (EF)} = \left[\frac{\text{EDD}^2\text{-ESD}^2}{\text{EDD}^2}\right] \quad (3)$$

$$\text{Tone} = \left(\frac{D_{MAX}\text{-EDD}}{D_{MAX}}\right) \times 100 \quad (4)$$

$$\text{Fractional Pump Flow (FPF)} = \text{EF} \cdot \text{FREQ} \quad (5)$$

where D_{MAX} represents the maximum passive diameter (obtained after incubation with calcium-free Krebs solution) at a given level of intraluminal pressure. When frequency was zero, a value for amplitude was omitted. The relative paucity of some amplitude data at low pressures in some

genotypes reflects the fact that this parameter could not be determined when frequency was zero. Each of the contractile parameters represented the average of all the recorded contractions during the measurement period at each intraluminal pressure.

Analysis of pressure-induced chronotropy

Quantification of the frequency-pressure (F-P) relationship for comparisons across genotypes required additional analysis steps, as illustrated in Fig. 1. Raw recordings of pressure and diameter (Fig. 1A) show the responses of a WT popliteal vessel to descending pressure steps from 5 to 0.5 cmH_2O, with the average frequency stated for each pressure. The frequency data were then plotted as a function of pressure (Fig. 1B). As evident from the behavior of this representative vessel, frequency tended to plateau above 5 cmH_2O, so the subset of data in which the response was nearly linear over the pressure range 0.5-5 cmH_2O was fitted with a first-order polynomial to obtain the slope and intercept (Fig. 1C). As an alternative method, we considered calculating the ratio of the respective contraction frequencies at 0.5 and 5 cmH_2O; however, in many cases no contractions occurred at P = 0.5 cmH_2O, which would equate to a ratio of infinity. To avoid this problem, we computed the difference (ΔF) between the frequencies at 5 and 0.5 cmH_2O. This approach gave consistent values that, like the slope, could detect blunting of the F-P relationship, but in essentially every case the results matched those of the curve fitting procedure; thus, only the F-P slope was used for statistical analyses and shown in subsequent figure plots. To enable a more comprehensive assessment of contractile function, full plots of amplitude, frequency, FPF and tone were also plotted as a function of pressure for each genotype (Fig. 1D).

FACS

Inguinal-axillary lymphatic vessels from tamoxifen-treated Myh11-CreER^{T2};*mTmG$^{f/f}$ and* Myh11-CreER^{T2};*Ano1$^{f/f}$*;*mTmG$^{f/f}$*mice were dissected and cleaned of fat and connective tissue as described previously (Zawieja *et al.*, 2018a). Cleaned vessel segments were transferred to a 1-ml tube of low-Ca^{2+} PSS containing (in mM): 137 NaCl, 5.0 KCl, 0.1$CaCl_2$, 1.0 $MgCl_2$, 10 HEPES, 10 Glucose, and 1 mg/ml BSA at room temperature for 10 min. The solution was decanted and replaced with a similar solution containing 26 U/ml papain (Sigma, St. Louis, MO) and 1 mg/ml dithioerythritol. The vessels were incubated for 30 min at 37°C with occasional agitation, then transferred to a new tube containing low-Ca^{2+} PSS containing 25 mg/ml collagenase H (FALGPA U/ml, Sigma), 0.7 mg/ml collagenase F (Sigma), 20 mg/ml trypsin inhibitor (Sigma), 1mg/ml elastase (Worthington), and incubated for 6 min at 37°C. The dispersed cells were sedimented by centrifugation (300 g, 4 min), resuspended in 0.6 ml PSS containing 1mM Ca solution, and filtered through a 35-µm mesh nylon filter to obtain a single cell suspension. GFP+ LMCs were sorted by fluorescence-activated cell sorting (FACS) using a Beckman-Coulter MoFlo XDP instrument with excitation laser (488 nm) and emission filter (530 ± 40 nm), a 70 µm nozzle, a sheath pressure of 45 psi and sort rate of 100 events per second. Sorting was performed at the Cell and Immunobiology Core facility at the University of Missouri.

RNA isolation and quantitative, real-time PCR

Total RNA was extracted from FACS-sorted cells using the Arcturus PicoPure RNA isolation kit (ThermoFisher Scientific, Waltham, MA) with on-column DNase I treatment (Qiagen, Valencia, CA) according to manufacturer's instructions. RNA was eluted with nuclease-free water. Purified RNA was transcribed into cDNA using High-Capacity cDNA Reverse Transcription kit (ThermoFisher Scientific, Waltham, MA). Real-time PCR (qPCR) was performed on cDNAs prepared from each sample using 2x PrimeTime Gene Expression Master Mix (IDT, Coralville, IA) with predesigned TaqMan probes as listed in Suppl. Table 1 (IDT, Coralville, IA). Real-time PCR protocols were as follows: preheating at 95°C for 3 min, 45 cycles of two-step cycling of denaturation at 95°C for 15 sec and annealing/extension steps of 30 sec at 60°C. Data collection was carried out using a Bio-Rad CFX 96 Real-Time Detection System (software version Bio-Rad CFX Manager 3.1; Bio-Rad, Hercules, CA, USA). For analysis, the result was expressed as a ratio of target gene/reference gene (β-actin).

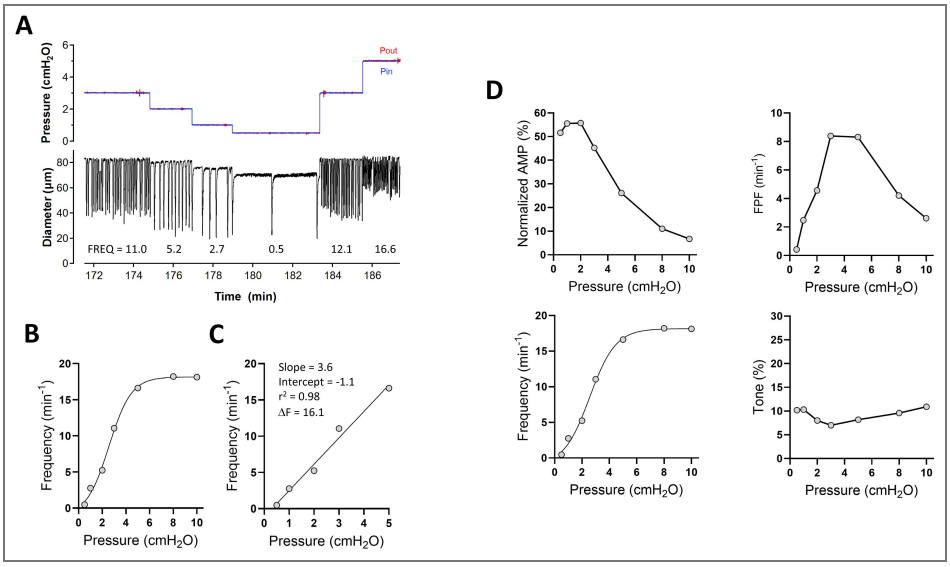

Figure 1. Quantification of the F-P relationship.

Steps for quantitative assessment of pressure-induced chronotropy. **A**) Representative recording of pressure and diameter changes in a WT popliteal lymphatic vessel during inflow (Pin) and outflow (Pout) pressure steps between 0.5 and 5 cmH_2O. Frequencies stated at the bottom of the trace were determined off-line using a custom peak detection program written in LabVIEW. **B**) Plot of frequency vs pressure for the vessel in A, showing how frequency reaches a plateau above 5 cmH_2O. **C**) Fit of the frequency data with a first-order equation and calculation of the frequency difference (ΔF) between 5 and 0.5 cmH_2O. **D**) Summary of contraction data for this representative WT vessel over the stated pressure range; see Methods for description of parameter calculations.

scRNAseq analysis

A total of 10 *Rosa26mTmG* mice (5 males and 5 females), without Cre and without tamoxifen treatment were used for scRNAseq analysis. Inguinal-axillary lymphatic vessels (IALVs) from both sides of each mouse were isolated and cleaned of connective and adipose tissue. The pooled vessels were digested into a single cell suspension and the cells were kept on ice until all tissues had been processed. Cells from all vessels were combined and sorted for tdTomato expression to remove debris and concentrate the cells for downstream single cell 3' RNA-Seq libraries creation with 10x Genomics Chromium Chip and Chromium Next GEM Single Cell 3' RNA-Seq reagents (Zawieja *et al*., 2025). Samples were sequenced with the NovaSeq 6000 S4-PE100 flow cell.

Mus musculus genome GRCm39 and annotation GTF (v106) from Ensembl (*https://useast.ensembl.org/Mus_musculus/Info/Index*) were used to build the reference index and the reads were processed using Cell Ranger (v7.0.1) using the default parameters. The quality control and filtering steps were performed using R (v4.2.1; *https://www.r-project.org/*). Ambient RNA was removed from the Cell Ranger output with SoupX (Young & Behjati, 2020). A doublet score for each cell was estimated using scDBlFinder [v1.12.0; (Germain *et al*., 2021)]. Non-expressed genes (sum zero across all samples) and low-quality cells (>10% mitochondrial genes, < 500 genes, < 1,000 UMIs per cell and doublet score <0.5) were removed with custom R scripts. Cells passing filtering were normalized/scaled (SCTransformation), dimensionally reduced (t-distributed stochastic neighbor embedding (t-SNE), uniform manifold approximation and projection (UMAP)) clustered, and hierarchically analyzed with Seurat (Hao *et al*., 2021; Hao *et al*., 2024) using the default parameters. Marker gene expression profile on cell clusters and gene co-expression were visualized using Seurat and ShinyCell R app (Ouyang et al., 2021 PMID: 33774659). The raw scRNAseq dataset is available on the NIH GEO #GSE277843 (eLIFE ref).

Solutions and chemicals

Krebs buffer contained: 146.9 mM NaCl, 4.7 mM KCl, 2 mM $CaCl_2{\cdot}2H_2O$, 1.2 mM $MgSO_4$, 1.2 mM $NaH_2PO_4{\cdot}H_2O$, 3 mM $NaHCO_3$, 1.5 mM Na-HEPES, and 5 mM D-glucose (pH = 7.4). An identical buffer was prepared with the addition of 0.5% bovine serum albumin ("Krebs-BSA"). During cannulation Krebs-BSA buffer was present both luminally and abluminally; however, during the experiment the abluminal solution was constantly exchanged with plain Krebs. Ca^{2+}-free Krebs was Krebs with 3 mM EGTA replacing $CaCl_2{\cdot}2H_2O$. All chemicals were obtained from Sigma-Aldrich (St. Louis, MO), with the following exceptions: BSA (US Biochemicals; Cleveland, OH), $MgSO_4$ and Na-HEPES (ThermoFisher Scientific; Pittsburgh, PA), ivabradine, zatebradine and losartan (Tocris). Amiloride, benzamil, ivabradine, zatebradine, $BaCl_2$ and losartan were dissolved in water to make stock solutions. Ani9, tranilast and SET2 were dissolved in DMSO to make stock solutions. Each inhibitor was then further diluted in Krebs solution to reach the final concentrations stated.

Statistical analysis

The data were analyzed in LabVIEW, compiled in Excel and statistical analyses were performed using Prism (v.10.2; Graphpad, San Diego, CA). Statistical differences in the slopes of the F-P relationships between two groups were assessed by an unpaired, two-tailed t-test, and differences between three or more groups were tested using a one-way ANOVA with Dunnett's post-hoc tests. Comparisons between contraction parameters as a function of pressure were made using two-way or mixed-model ANOVAs with repeated measures and Sidák's post-hoc tests. Data are plotted as mean ± SEM. Significance levels (compared to the control group) are either stated or indicated as follows: *p<0.05; **p<0.01; ***p<0.001; ****p<0.0001; "n.s." p≥0.05, with the color-coding of the symbols matching the respective group. In the figure legends, N refers to the number of animals and n refers to the number of vessels per group.

Results

Role of ANO1 in pressure-induced chronotropy

Single cell RNAseq analyses from dissected IALVs revealed 19 distinct cell clusters (Fig. 2A), segregating into prominent clusters/subclusters of lymphatic endothelial cells (LECs), LMCs, adventitial cells (AdvCs) and immune cells. Further analysis confirmed that *Ano1* was expressed at moderate levels (relative to *Acta2*) in >75% of LMCs and to a lesser extent in AdvCs, but not in LECs (Fig. 2A). AdvCs contained subclusters of adventitial fibroblasts and other cell types expressing multiple stem cell markers (Zawieja *et al*., 2019).

Previously, we reported that ANO1 inhibition or SM-specific *Ano1* deletion caused a nearly complete abrogation of pressure-induced chronotropy in mouse IALVs. However, the contraction frequency of IALVs changes only ~1.7 fold over the pressure range from 0.5 to 10 cmH_2O (Zawieja *et al*., 2019), compared to the much larger dynamic range (≥ 10-fold) characteristic of popliteal lymphatics (Fig. 1). Thus, we used popliteal lymphatics throughout this study to assess pressure-induced chronotropy, in anticipation that we would be able to detect even subtle changes in the response after deletion of specific genes. The F-P analysis for 20 WT popliteal lymphatic vessels is shown in Fig. 2. C57Bl/6 mice served as the WT control group for many comparisons because all transgenic strains used in the present study (with one exception) were derived from, or backcrossed into, that background. The average slope (± SEM) of the F-P relationship between 0.5 and 5 cmH_2O was 2.8 ± 0.3 for WT vessels (Fig. 2B), equating to an average frequency difference of 12.1 ± 1.0 contractions·min^{-1} over that pressure range. The average r^2 value for the linear regressions was 0.93 ± 0.02, indicating a consistently high quality of the curve fits and confirming that the slope was approximately linear between 0.5 and 5 cmH_2O. The role of ANO1 in pressure-induced chronotropy of mouse popliteal lymphatic vessels was then tested after pharmacologic inhibition of ANO1 with Ani9, one of the most selective small molecule inhibitors of ANO1 (Hwang *et al*., 2016). Initial assessment of the Ani9 concentration-response relationship (from 30 nM to 10 μM) in WT popliteal vessels revealed that 3 μM Ani9, the concentration previously used to inhibit ANO1 in IALVs (Zawieja *et al*., 2019; Zawieja *et al*., 2023), did indeed reduce the basal contraction frequency of popliteal lymphatics (in the lower pressure range), but also caused a loss of tone and marked reduction in their contraction amplitude (not shown)—suggestive of possible off-target effects; therefore, for subsequent F-P protocols we used a lower concentration (1 μM) of Ani9, which had insignificant effects on contraction amplitude and tone (Fig. 2C) but significantly reduced the average slope of the F-P relationship from 2.8 ± 0.3 to 0.3 ± 0.2 ($p<0.001$; Fig. 2B).

We then tested the effects of SM-specific *Ano1* deletion by comparing the F-P relationship of popliteal lymphatic vessels from tamoxifen-treated Myh11-$CreER^{T2}$;$Ano1^{f/f}$ (*Ano1 smKO*) mice to $Ano1^{f/f}$ control mice. The results are also shown in Fig. 2B. The average slope of the F-P relationship between 0.5 and 5 cmH_2O for *Ano1 smKO* vessels was 0.4 ± 0.2, significantly lower ($p<0.001$) than that (2.8 ± 0.2) for $Ano1^{f/f}$ vessels. Complete sets of contraction data for untreated and Ani9-treated WT popliteal lymphatics, Myh11-$CreER^{T2}$;$Ano1^{f/f}$ and $Ano1^{f/f}$popliteal vessels, are shown in Fig. 2C. The frequency of Ani9-treated vessels was significantly reduced at most pressures but increased at higher pressures. Normalized contraction amplitudes were unchanged by Ani9. Tone was slightly but not significantly higher in Ani9-treated vessels. After *Ano1* deletion, frequency was reduced to <3 contractions·min^{-1} at all pressures, in contrast to Ani9-treated WT vessels in which frequency was comparably reduced at low pressures but not at elevated pressures (Fig. 2C). *Ano1 smKO* vessels had significantly elevated levels of tone at 5 of 7 pressures, suggesting that Ani9 treatment may have interfered with tone development in a way that *Ano1* deletion did not. Collectively, these results show that deletion / inhibition of ANO1 significantly impaired pressure-induced chronotropy in popliteal lymphatic vessels; however, SM-specific *Ano1* deletion failed to completely abolish spontaneous contractions in 16 of 21 *Ano1 smKO* vessels. To test the possibility that residual pacemaking activity in *Ano1 smKO* vessels might be due to incomplete recombination by the inducible Myh11-$CreER^{T2}$ driver, *Ano1* mRNA levels in IALVs were quantified using qPCR analysis. Smooth muscle cells were digested from IALVs of

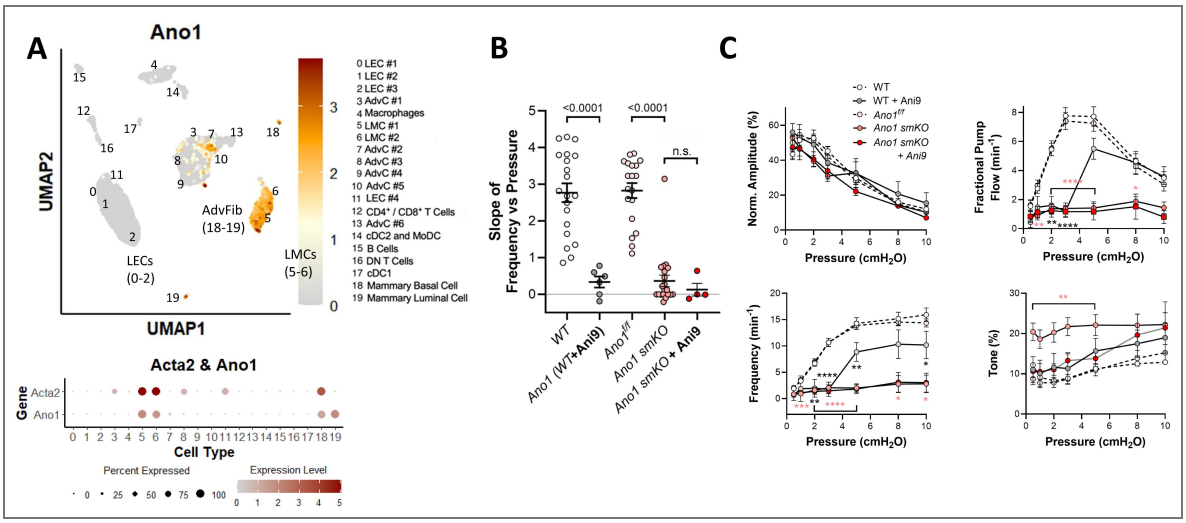

Figure 2. Consequences of ANO1 deletion and/or inhibition.

A) UMAP plot of *Ano1* expression in the various cell populations within the walls of murine IALVs that were thoroughly cleaned prior to dissociation and scRNAseq analysis, as described in (Zawieja *et al*., 2025). The LMC cluster (composed of at least two subclusters of 978 cells) was identified by the expression of canonical smooth muscle cell markers *Acta2* (SM α-actin), *Myh11* (myosin heavy chain 11), *Itga8* (integrin alpha 8). Gray color in this and subsequent figures represents *Acta2* expression, red/brown in this panel indicates *Ano1* expression. Bubble plot shows Ano1 expression in the LMC and other cell clusters in terms of percent cells in an individual cluster expressing *Ano1* (size of dot) and the *Ano1* expression level relative to *Acta2* (color of dot). **B**) Slope of frequency vs pressure (F-P) for WT (C57Bl/6) vessels with / without treatment by the ANO1 inhibitor Ani9 (1 μM), for *Ano1*$^{f/f}$ control vessels, for *Ano1 smKO* vessels and for the latter treated with Ani9. **C**) Summary plots of contraction parameters as a function of pressure for the 5 respective groups of vessels. WT N=15, n=20; WT+Ani9 N=5, n=6; *Ano1 smKO* N=14, n=23; *Ano1*$^{f/f}$ N=8, n=16.

Myh11-CreER^{T2};*mTmG*$^{f/f}$or Myh11-CreER^{T2};*mTmG*$^{f/f}$;*Ano1*$^{f/f}$ mice and purified by FACS using the GFP signal. *Ano1* message (referenced to α-actin levels) in LMCs from Myh11-CreER^{T2};*mTmG*$^{f/f}$;*Ano1*$^{f/f}$ vessels was undetectable compared to that in LMCs from Myh11-CreER^{T2};*mTmG*$^{f/f}$ vessels (0 ± 0 and 1006 ± 80, respectively; mean ± SD, n=3). As a further test for possible residual ANO1 activity in *Ano1 smKO* vessels, we treated another group of *Ano1 smKO* vessels with Ani9 (1 μM), and those results are shown in Fig. 2B-C. Pacemaking activity persisted even after combined deletion and inhibition of ANO1, without significant further reductions in frequency at any pressure, suggesting that residual pacemaking in *Ano1* KO vessels was *not* due to incomplete ANO1 knock down. Collectively, these results point to ANO1 as the major component of pressure-induced lymphatic chronotropy but also to the involvement of one or more additional mechanisms, possibly involving other LMC ion channels.

Role of PIEZO1

PIEZO1 and PIEZO2 are two ion channels that satisfy the full set of criteria for true mechanosensitivity (Coste *et al*., 2010; Davis *et al*., 2023c). PIEZO2 is expressed primarily in neurons (Woo *et al*., 2014; Woo *et al*., 2015) whereas PIEZO1 is more widely expressed (Murthy *et al*., 2017). PIEZO1 is critically important for shear-stress induced Ca^{2+} signaling in endothelium (Li *et al*., 2014a), for lymphatic valve and vessel development (Nonomura *et al*., 2018; Choi *et al*., 2019; Choi *et al*., 2024) and for hypertension-dependent arterial wall remodeling (Retailleau *et al*., 2015). The role of PIEZO1 in the arterial myogenic response has not been systematically tested, except for a single report showing that SM-specific *Piezo1* deletion did not alter myogenic tone development in either caudal and rostral cerebellar arteries of mice [Suppl. Figs. 2-3 in (Retailleau *et al*., 2015)]. The possible involvement of PIEZO1 in lymphatic vessel contractility has not been reported. Our scRNAseq analysis revealed strong expression of *Piezo1* message in LECs but very weak expression in LMCs (Fig. 3A). *Piezo2* expression was barely detectable in either cell type. Popliteal lymphatic vessels from Myh11-CreER^{T2};*Piezo1*$^{f/f}$ (*Piezo1 smKO*) and *Piezo1*$^{f/f}$control mice were subjected to the protocol for assessing pressure-induced chronotropy. However, the data revealed no significant difference in the F-P slope between *Piezo1 smKO* vessels and *Piezo1*$^{f/f}$ control vessels (Fig. 3B), suggesting that PIEZO1 channels in LMCs are not required for pressure-induced lymphatic chronotropy. As a further test, we used Nestin-Cre to generate Nestin-Cre;*Piezo1*$^{f/f}$ *(Piezo1 nestinKO)* mice with constitutive deletion of *Piezo1* both in smooth muscle and other cells expressing intermediate filaments. An analysis of vessel responses from *Piezo1 nestinKO* mice indicated that there was no significant impairment in pressure-induced chronotropy (Fig. 3B). Although we did not suspect the endothelium would be involved in pressure-induced chronotropy, we also generated and tested Prox1-CreER^{T2};*Piezo1*$^{f/f}$ *(Piezo1 lecKO)* mice. As expected, there was no significant difference in the average F-P slope of vessels from *Piezo1 lecKO* mice compared to tamoxifen-treated *Piezo1*$^{f/f}$ controls (Fig. 3B). Complete sets of contraction data for popliteal vessels from *Piezo1 smKO* are shown in Fig. 3C and revealed no significant differences in any of the lymphatic contractile parameters at any pressure compared to their floxed controls.

Roles of TRPC6 and TRPC3

TRPC6 is thought to be a mechanosensitive cation channel whose activation underlies pressure-induced constriction in cerebral arteries (Welsh *et al*., 2002). However, studies of other arteries from *Trpc6*$^{-/-}$ mice found either no differences from control vessels or even *enhanced* myogenic responsiveness (Dietrich *et al*., 2005; Schleifenbaum *et al*., 2014). Because global TRPC6 deletion results in compensatory upregulation of TRPC3 (Dietrich *et al*., 2005), a related TRPC family member with similar properties and which is also activated by DAG, it is possible that TRPC3 could compensate for loss of TRPC6. The expression patterns for TRPC6 and TRPC3, based on scRNAseq analyses, are shown in Fig. 4A. TRPC6 was expressed at modest levels in ~50% of LMCs and was almost exclusively confined to LMCs. TRPC3 was expressed at very low levels in only a few LMCs (from control mice). We tested the effects of global TRPC6 deletion (*Trpc6*$^{-/-}$), global TRPC3 deletion (*Trpc3*$^{-/-}$) and global deletion of both isoforms (*Trpc6*$^{-/-}$;*Trpc3*$^{-/-}$) on pressure-induced lymphatic chronotropy. As these mice were all generated in the SV129

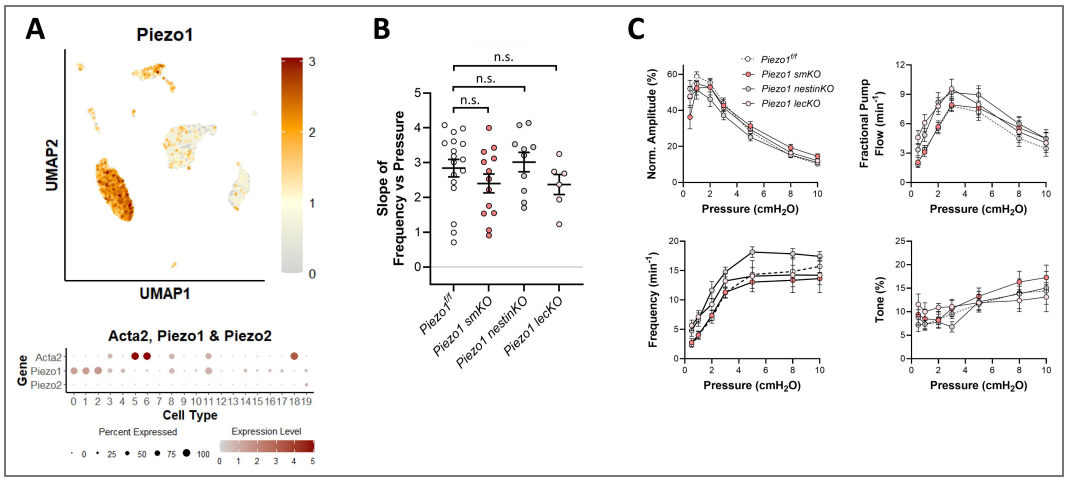

Figure 3. **Consequences of *Piezo1* deletion.**

A) UMAP and bubble plots of *Piezo1 and Piezo2* expression in the various IALV cell clusters. **B**) Slope of F-P relationship for popliteal lymphatics from *Piezo1*$^{f/f}$, *Piezo1 smKO*, *Piezo1 nestin KO*, *Piezo1 lecKO* mice. **C**) Summary plots of contraction parameters as a function of pressure for the 4 respective groups of vessels. *Piezo1*$^{f/f}$ N=9, n=17; *Piezo1 smKO* N=7, n=13; *Piezo1 nestin KO* N=5, n=10; *Piezo1 lecKO* N=5, n=6.

background, control measurements were performed on popliteal vessels from SV129 mice, which showed a *lower* average F-P slope than WT (C57Bl/6) popliteal vessels. There were no significant differences in F-P slope between SV129 controls and *Trpc6*$^{-/-}$ or *Trpc3*$^{-/-}$ vessels, but the F-P slope of *Trpc6*$^{-/-}$*;Trpc3*$^{-/-}$ vessels was significantly *higher* than that of the SV129 controls (Fig. 4B). Complete sets of contraction data for *Trpc6*$^{-/-}$*;Trpc3*$^{-/-}$ vessels, compared to their *SV129* controls, are shown in Fig. 4C. *Trpc6*$^{-/-}$*;Trpc3*$^{-/-}$double knock-out vessels had significantly impaired contraction amplitudes at several pressures and *increased* frequencies and *increased* levels of tone at most pressures. However, relevant to the main objective of this study, there were no significant *impairments* in pressure-induced chronotropy in vessels deficient in TRPC6, TRPC3 or both TRPC6 and TRPC3 (Fig. 4B-C).

Role of TRPM4

Multiple studies have implicated TRPM4 channels in the arterial myogenic response (Gonzales & Earley, 2013; Earley & Brayden, 2015), but to date no published studies have examined the role of TRPM4 in lymphatic vessel contractility. scRNAseq analysis revealed that *Trpm4* was expressed at modest levels in only ~10% of LMCs, and in a subset of LECs, but at higher levels in some AdvCs (Fig. 5A). We tested the role of TRPM4 in pressure-induced lymphatic chronotropy by comparing the responses of Myh11-CreER^{T2}*;Trpm4*$^{f/f}$ vessels to *Trpm4*$^{f/f}$vessels. The lack of significant reductions in F-P slope of *Trpm4 smKO* vessels (Fig. 5B) suggests that TRPM4 is not required for pressure-induced lymphatic chronotropy. Contraction data comparing *Trpm4 smKO* vessels to *Trpm4*$^{f/f}$ popliteal vessels are shown in Fig. 4C. There were no significant differences between the contraction parameters of *Trpm4 smKO* and *Trpm4*$^{f/f}$ vessels at any pressure.

Role of PKD2

Studies by Jaggar and colleagues indicate that SM-specific deletion of PKD2 attenuates pressure-induced depolarization and myogenic tone in rat pial arteries (Narayanan *et al*., 2013) and blunts pressure-induced constriction in hindlimb arteries (Bulley *et al*., 2018). The roles of PKD2/2 channels in lymphatic vessel contractility are not known. scRNAseq analysis revealed modest *Pkd2* and *Pkd1* expression in LMCs and AdvCs (Fig. 6A). We tested the possible involvement of PKD2 channels in pressure-induced lymphatic chronotropy by comparing the responses of Myh11-CreER^{T2}*;Pkd2*$^{f/f}$(*Pkd2 smKO*) vessels to *Pkd2*$^{f/f}$ vessels (Fig. 6B). The lack of a significant reduction in the F-P slope for *Pkd2 smKO* vessels suggests that PKD2 is not required for pressure-induced lymphatic chronotropy. Contraction data comparing *Pkd2 smKO* vessels to *Pkd2*$^{f/f}$ popliteal vessels are shown in Fig. 6C. There were no significant differences between the contraction parameters of *Pkd2 smKO* and *Pkd2*$^{f/f}$ vessels at any pressure.

Role of TRPV4

In the blood vasculature, TPRV4 has been studied extensively in the context of Ca^{2+} influx pathways in endothelium (Chen & Sonkusare, 2020). However, TRPV4 is also expressed in VSM cells of some arteries (Mercado *et al*., 2014) and one report indicates that pharmacological inhibition of TRPV4 channels blunts pressure-induced VSM cell depolarization and myogenic vasoconstriction of preglomerular arteries from neonatal pigs (Soni *et al*., 2017). Our scRNAseq analysis revealed that TRPV4 was largely undetectable in LMCs but expressed at higher levels in almost all LECs, macrophages and some AdvCs (Fig. 7A). Nonetheless, we tested the role of TRPV4 channels in pressure-induced lymphatic chronotropy by comparing the responses of Myh11-CreER^{T2}*;Trpv4*$^{f/f}$ vessels to *Trpv4*$^{f/f}$ vessels. The lack of a significant reduction in the F-P slope for *Trpv4 smKO* vessels suggests that TRPV4 is not required for pressure-induced lymphatic chronotropy (Fig. 7B). Contraction data comparing *Trpv4 smKO* and *Trpv4*$^{f/f}$ popliteal vessels are shown in Fig. 7C. Contraction amplitude was impaired at several pressures in *Trpv4 smKO* vessels, suggesting some involvement of TRPV4 channels in control of contractile strength, possibly as a result of macrophage-released products (Schulz *et al*., 2025). Frequency was significantly different at two lower pressures in *Trpv4 smKO* vessels (Fig. 7C), where it was *elevated* rather than reduced. We also tested the F-P relationship in *Trpv4*$^{-/-}$ (global KO) vessels

Figure 4. **Consequences of *Trpc6* and/or *Trpc3* deletion.**

A) UMAP and bubble plots of *Trpc6 and Trpc3* expression in the various IALV cell clusters. **B**) Slope of F-P relationship for popliteal lymphatics from SV129 controls, *Trpc6*$^{-/-}$, *Trpc3*$^{-/-}$ *and Trpc6*$^{-/-}$;*Trpc3*$^{-/-}$ mice. **C**) Summary plots of contraction parameters as a function of pressure for the 4 respective groups of vessels. SV129 control N=8, n=11; *Trpc6*$^{-/-}$ N=5, n=10; *Trpc3*$^{-/-}$ N=7, n=11; *Trpc6*$^{-/-}$;*Trpc3*$^{-/-}$ N=5, n=10.

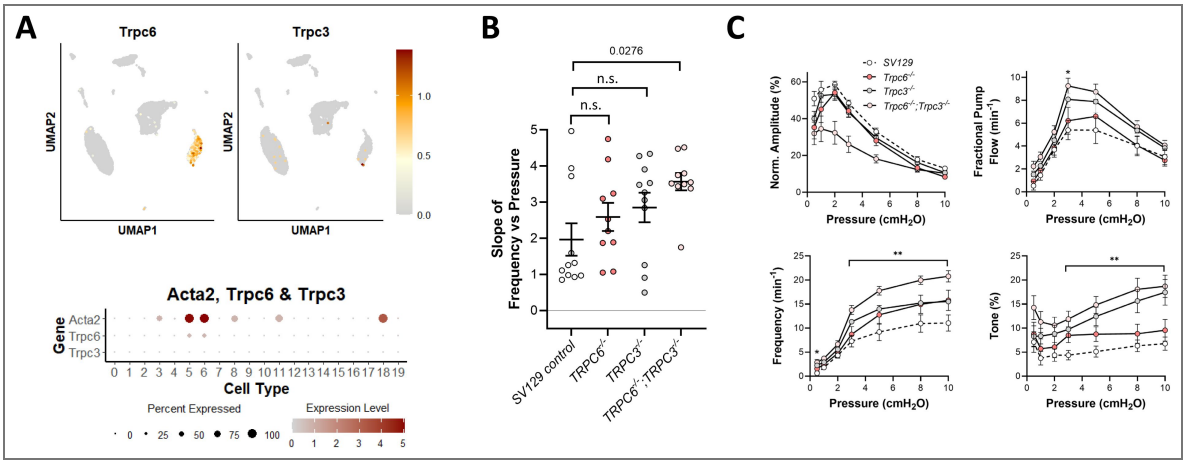

Figure 5. **Consequences of *Trpm4* deletion.**

A) UMAP and bubble plots of *Trpm4* expression in the various IALV cell clusters. **B**) Slope of F-P relationship for popliteal lymphatics from *Trpm4*$^{f/f}$ *and Trpm4 smKO* mice. **C**) Summary plots of contraction parameters as a function of pressure for the two respective groups of vessels. *Trpm4 smKO* N=6, n=13; *Trpm4*$^{f/f}$ N=4, n=7.

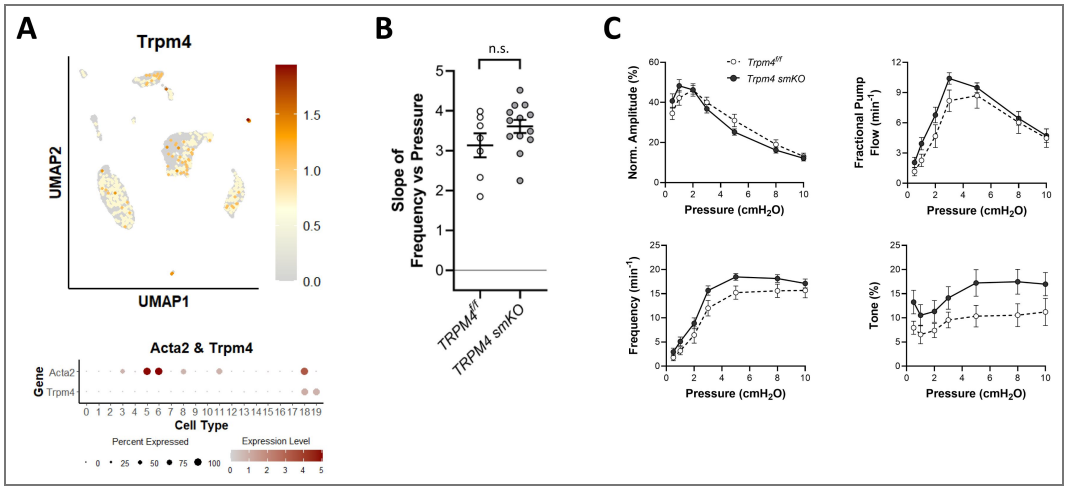

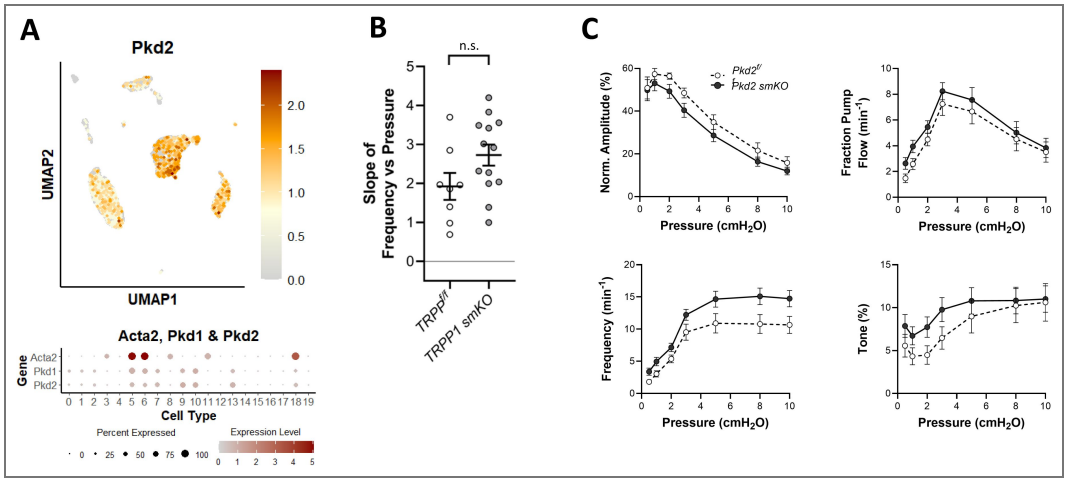

Figure 6. **Consequences of *Pkd2* (TRPP1) deletion.**

UMAP and bubble plots of *Pkd2* expression in the various IALV cell clusters. **B**) Slope of F-P relationship for popliteal lymphatics from *Pkd2 f/f and Pkd2 smKO* mice. **C**) Summary plots of contraction parameters as a function of pressure for the two respective groups of vessels. *Pkd2 smKO* N=6, n=13; *Pkd2 f/f* N=4, n=8.

and confirmed that there was no significant impairment in pressure-induced lymphatic chronotropy (average slope = 2.7 ± 0.2; n=18) compared to WT vessels (average slope = 2.8 ± 0.3; data not shown). Collectively, these results indicate that TRPV4 channels are not required for pressure-induced lymphatic chronotropy.

Role of TRPV2

TRPV2 is an osmosensitive cation channel (Nilius & Droogmans, 2001). Down-regulation of TRPV2 expression in mouse aortic VSM cells reduced the amplitude of cation currents activated by hypotonic swelling (Muraki *et al*., 2003). In another study, application of a hypotonic bath solution stimulated TRPV2-like whole-cell cation currents and Ca^{2+} influx in VSMCs isolated from rat retinal arteries—responses that were attenuated by the TRPV2 inhibitor tranilast (McGahon *et al*., 2016). Additionally, the administration of tranilast to rat retinal arteries resulted in loss of pre-existing myogenic tone whereas pre-incubation with a TRPV2 blocking antibody prevented the development of myogenic tone (McGahon *et al*., 2016). Our scRNAseq analysis revealed that TRPV2 was highly expressed in 63% of *Myh11*-expressing LMCs (Fig. 8A). As we did not have access to TRPV2 null or floxed mice, we tested the potential role of TRPV2 channels in pressure-induced lymphatic chronotropy by bath application of tranilast (100 μM) to WT popliteal lymphatic vessels. There was no significant reduction in the F-P slope for tranilast-treated vessels (Fig. 8B). We also tested the effects of SET2, a recently reported TRPV2 inhibitor with a lower IC_{50} (460 nM) than tranilast. The application of SET2 (1 μM) caused a transient cessation of spontaneous contractions for 2-5 min in 5 of 6 vessels, but the contractions returned within 10 min in the continued presence of SET2. Subsequent pressure steps revealed that SET2 did not significantly alter the F-P slope (Fig. 8B). Contraction data comparing WT and tranilast-and SET2-treated WT popliteal vessels are shown in Figs. 8C. These results suggest that TRPV2 is not required for pressure-induced lymphatic chronotropy.

Role of ENaC

The epithelial Na^+ channel (ENaC), comprised of a heterotrimer under the expression of the genes *Scnn1a*, *Scnn1b*, *Scnn1g*, *Scnn1d*, is expressed in both the endothelial and smooth muscle layers of arteries. αENaC is the principal isoform in endothelium and studies of native epithelial or heterologous channels reconstituted into bilayers suggest that αENaC is intrinsically mechanosensitive (Price *et al*., 2000; Benos, 2004). Work from the Drummond laboratory suggests that the βENaC isoform is expressed in VSM cells and plays a critically important role in myogenic constriction (Drummond, 2012). However, our scRNAseq analysis revealed almost no expression of αENaC subunits in LMCs and only weak expression in the LEC population (Fig. 9A); βENaC was essentially undetectable. Nevertheless, we tested the possible role of ENaC in pressure-induced lymphatic chronotropy by administering two widely used ENaC inhibitors, amiloride and benzamil, to WT popliteal lymphatic vessels. The data in Fig. 9B show that neither amiloride nor benzamil, at concentrations known to inhibit arterial myogenic constriction [5 and 1 μM, respectively (Jernigan & Drummond, 2006)], caused a significant impairment in pressure-induced lymphatic chronotropy. Contraction data for amiloride- and benzamil-treated WT popliteal vessels are shown in Fig. 9C. Both ENaC inhibitors tended to impair contraction amplitude to some degree (significant only for amiloride), with benzamil also significantly increasing tone at almost all pressure levels. However, the F-P relationships were nearly identical between WT and amiloride- or benzamil-treated vessels, reinforcing the conclusion that ENaC is not involved in pressure-induced lymphatic chronotropy.

Role of NCX1

The sodium-calcium exchanger (NCX) has a well-documented role in controlling the pacemaker activity of sinoatrial nodal cells, where it couples SR calcium oscillations, termed local calcium releases (LCRs) caused by calcium movement through ryanodine channels (Vinogradova *et al*., 2004; Vinogradova *et al*., 2005), to AP ignition. LCRs may occur throughout diastole (Monfredi *et al*., 2013), but their role is particularly critical in late diastole where LCRs activate NCX and

Figure 7. **Consequences of *Trpv4* deletion.**

UMAP and bubble plots of *Trpv4* expression in the various IALV cell clusters. **B**) Slope of F-P relationship for popliteal lymphatics from *Trpv4$^{f/f}$ and Trpv4 smKO* mice. **C**) Summary plots of contraction parameters as a function of pressure for the two respective groups of vessels. *TRPV4 smKO* N=5, n=10; *TRPV4$^{f/f}$* N=3, n=7.

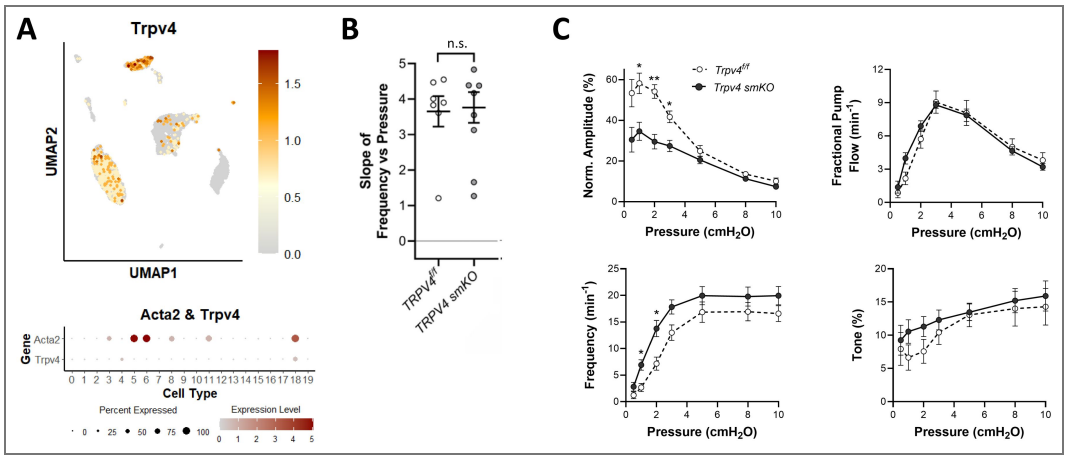

Figure 8. **Consequences of Trpv2 inhibition.**

UMAP and bubble plots of *Trpv2* expression in the various IALV cell clusters. **B**) Slope of F-P relationship for popliteal lymphatics from WT mice with/without treatment with the TRPV2 inhibitors tranilast (10 μM) and SET2 (1 μM). **C**) Summary plots of contraction parameters as a function of pressure for the three respective groups of vessels. WT+tranilast N=5, n=10; WT+SET2 N=3, n=6.

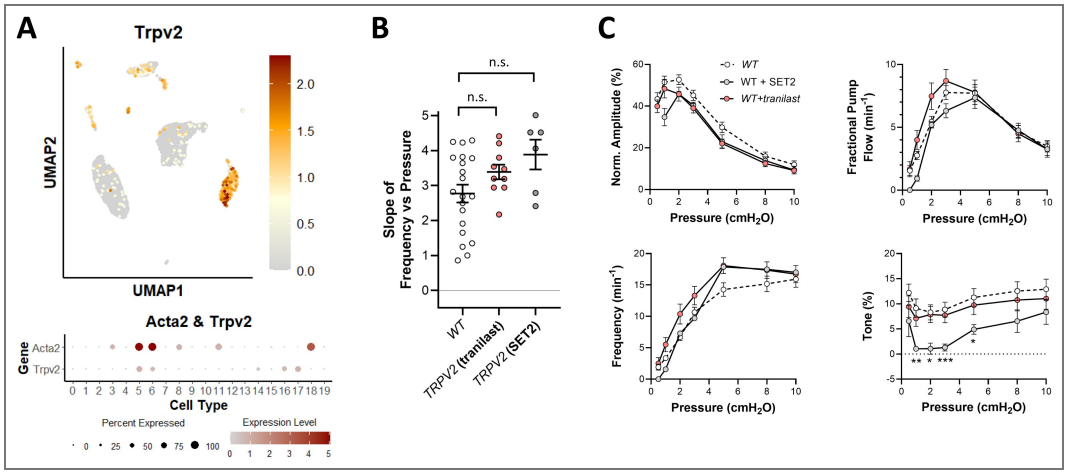

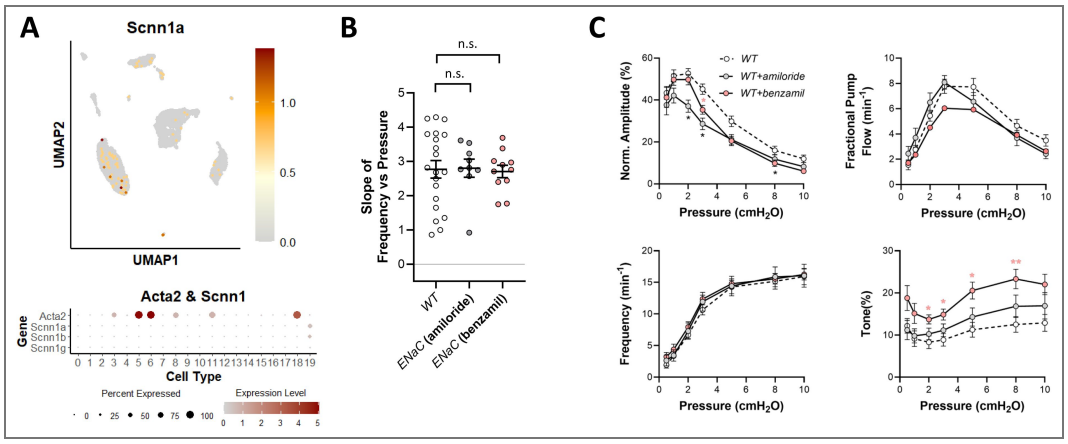

Figure 9. Consequences of ENaC inhibition.

UMAP and bubble plots of *ENaC* subsunit expression in the various IALV cell clusters. **B**) Slope of F-P relationship for popliteal lymphatics from WT mice with/without treatment with the ENaC inhibitors amiloride (5 μM) and benzamil (1 μM). WT N=15, n=20, WT+amiloride N=5, n=9; WT+benzamil N=6, n=11.

the ensuing addition of inward current, and positive feedback of further calcium influx through L-type channels, provides sufficient depolarization to cross the voltage threshold for initiating AP firing (Bogdanov *et al*., 2001; Lyashkov *et al*., 2018b). This process is possibly analogous to the electrophysiological pacemaking mechanism in LMCs. scRNAseq analysis revealed strong expression of *Slc8a*, which encodes NCX1, in >80% of both LMCs and expression was also noted in LECs and some immune cells (Fig. 10A). We tested the role of NCX1 in pressure-induced chronotropy by comparing the responses of Myh11-CreER^{T2};*Slc8a1*$^{f/f}$ (*Slc8a1 smKO*) and *Slc8a1*$^{f/f}$ vessels. The lack of a significant reduction in the F-P slope for *Slc8a1 smKO* vessels suggests that NCX1 is not required for pressure-induced lymphatic chronotropy (Fig. 10B). Contraction data for *Slc8a1 smKO* and *Slc8a1*$^{f/f}$ popliteal vessels are shown in Fig. 10C and reveal no significant differences between the contraction parameters of *Slc8a1 smKO* and *Slc8a1*$^{f/f}$ vessels.

Role of HCN

HCN (Hyperpolarization-activated cyclic-nucleotide-gated) channels contribute an inward "funny" current (I_f) to the diastolic pacemaking potential of sinoatrial node cells (Accili *et al*., 2002) and are also involved in the intrinsic rhythmicity of bladder and uterine smooth muscle (Alotaibi *et al*., 2017; Mader *et al*., 2018). In LMCs they could potentially contribute to diastolic depolarization. The HCN blockers CsCl, ZD7288 and ivabradine all lower the rate of spontaneous contractions of lymphatic vessels in rat diaphragm (Negrini *et al*., 2016), but inhibition requires substantially higher concentrations than the documented IC_{50} values for HCN channel blockade [see discussion in (Davis & Zawieja, 2024)]. In contrast, all three inhibitors *increase* the spontaneous contraction frequency of human lymphatic vessels at concentrations near or slightly higher than the IC_{50} values for HCN inhibition (Majgaard *et al*., 2022), suggesting off-target effects in some lymphatic vessels. Our scRNAseq analysis revealed essentially no expression of any of the four HCN isoforms in LMCs (Fig. 11A), however it is possible the expression is too low to detect without deep sequencing. Due to the proven role of HCN channels in cardiac pacemaking, we tested the role of HCN channels in pressure-induced lymphatic chronotropy of WT mouse popliteal lymphatics using the HCN inhibitor ivabradine (at a concentration of 3 μM, which is slightly higher than the IC_{50} of 2.5 μM), and the more effective inhibitor, zatebradine, at a concentration of 3 μM (IC_{50} = 480 nM). The lack of significant reductions in the F-P slope for ivabradine- or zatebradine-treated WT vessels suggests that HCN channels are not required for pressure-induced lymphatic chronotropy (Fig. 11B). Contraction data for ivabradine- and zatebradine-treated WT vessels are shown in Fig. 11C and reveal no substantial differences from WT vessels, except for a single pressure in which each HCN channel inhibitor actually *increased* the contraction frequency. Collectively, these results recapitulate the findings of Majgaard et al (Majgaard *et al*., 2022) and reinforce the conclusion that HCN channels are not required for pressure-induced lymphatic chronotropy.

Role of Kv7.4

Kv7 channels are activated at more negative membrane potentials than Kv1-family delayed rectifier K^+ channels and thus are implicated in control of VSMC excitability near the resting membrane potential (Yeung & Greenwood, 2005; Zhong *et al*., 2010; Mani & Byron, 2011). The Kv7 blocker XE991 enhances myogenic tone in isolated mesenteric and renal arteries and hypotonic swelling suppresses an XE991-sensitive Kv current in patch-clamped VSM cells (Schleifenbaum *et al*., 2014). The collective implication from these studies is that mechanosensitive *inhibition* of Kv7.4 may increase VSM excitability. The effects of Kv7 channel inhibition on lymphatic function are unknown but the pan-Kv7 channel inhibitors linopirdine and XE991 cause concentration-dependent increases in lymphatic contraction frequency while the Kv7 activator ML-277 inhibits spontaneous lymphatic contractions (our unpublished observations in rat mesenteric lymphatic vessels). Our scRNAseq analysis revealed moderately strong expression of *Kcnq4* in >50% LMCs and in some AdvCs (Fig. 12A). We tested whether pressure-induced lymphatic chronotropy was altered in Myh11-CreER^{T2};*Kcnq4*$^{f/f}$ (*Kcnq4 smKO)* mice. However, the lack of a significant reduction in the F-P slope for *Kcnq4 smKO* vessels suggests that Kv7.4 channels

Figure 10. Consequences of *Slc8a1* (NCX1) deletion.

UMAP and bubble plots of *Slc8a1* expression in the various IALV cell clusters. **B**) Slope of F-P relationship for popliteal lymphatics from *Slc8a1*$^{f/f}$ *and Slc8a1 smKO* mice. **C**) Summary plots of contraction parameters as a function of pressure for the two respective groups of vessels. *Slc8a1*$^{f/f}$ N=7, n=12; *Slc8a1 smKO* N=7, n=13.

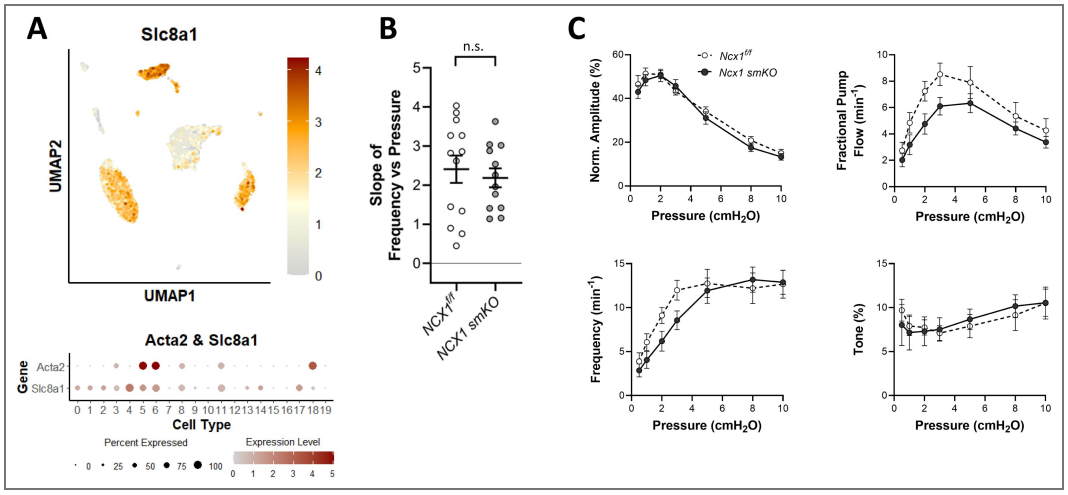

Figure 11. Consequences of HCN inhibition.

UMAP and bubble plots of *Hcn gene* family expression in the various IALV cell clusters. **B**) Slope of F-P relationship for popliteal lymphatics from WT mice with/without treatment with the HCN inhibitors ivabradine (3 μM) and zatebradine (3 μM). WT N=15, n=20, WT+zatebradine. N=5, n=10; WT+ivabradine N=5, n=10.

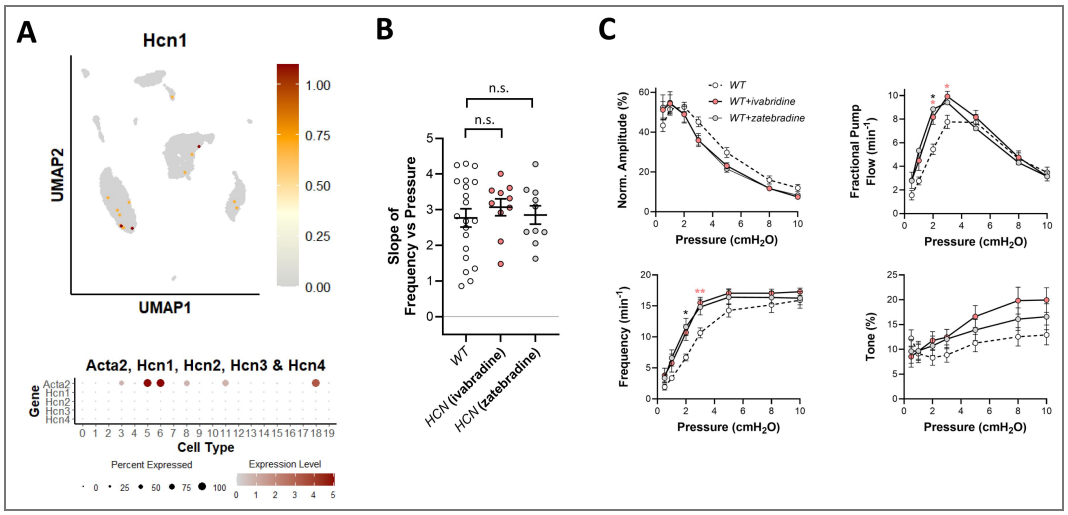

are not required for pressure-induced lymphatic chronotropy (Fig. 12B). Contraction data for *Kcnq4 smKO* and *WT* vessels are compared in Fig. 12C. There were no significant differences in any of the parameters at any pressure.

Role of Kir channels

Inwardly rectifying K^+ channels, including Kir2.1 and Kir2.2 which are encoded by *Kcnj2* and *Kcnj12* respectively, have been implicated in shear-stress-induced responses of arterial endothelium (Ahn *et al*., 2017) and swelling-induced currents in arterial smooth muscle cells (Sancho *et al*., 2019). However, their potential roles in controlling LMC membrane potential and pressure-induced lymphatic chronotropy are unknown. Our scRNAseq analysis revealed modest expression of *Kcnj8* (Kir6.1), an inward rectifier which forms the pore forming unit of the K_{ATP} channel, in >50% LMCs (Fig. 13A), but very little expression of *Kcnj2* or *Kcnj12* in LMCs. We previously showed that deletion of *Kcnj8* does not alter the F-P relationship in popliteal lymphatics (Davis *et al*., 2020). Here, we tested the effects of $BaCl_2$, a selective inhibitor of Kir2.1/2.2 at a concentration of 100 μM (Longden *et al*., 2017; Sancho *et al*., 2017; Sancho *et al*., 2019), on the F-P relationship of WT popliteal lymphatic vessels. Kir inhibition resulted in a significantly reduced slope of the F-P relationship compared to WT vessels (Fig. 13B), but the consistent effect of Ba^{2+} was to flatten the slope of the F-P relationship by substantially *increasing* the contraction frequency at low pressures while only slightly *increasing* the contraction frequency at elevated pressures (Fig. 13C). This contrasts with the effect of ANO1 inhibition or deletion: in the absence of ANO1 activity, the contraction frequency was significantly reduced at all pressures, particularly at low pressures (Fig. 2C). Thus, the inhibition of Kir channels does impair pressure-induced chronotropy but does so by differentially *elevating* contraction frequency as a function of pressure.

Roles of L- and T-type Ca^{2+} channels

The L-type, voltage-gated Ca^{2+} channel (Cav1.2) carries the majority of current contributing to the action potential in LMCs (van Helden, 1993; To *et al*., 2020). scRNAseq analysis confirmed that >90% of LMCs expressed message for the pore forming subunit of Cav1.2 (*Cacna1c*), along with other accessory subunits of the channel responsible for either gating characteristics (α2δ) or membrane targeting (β) (Fig. 14A). SM-specific knockout of *Cacna1*, using either the Myh11-$CreER^{T2}$ or Itga8-$CreER^{T2}$, eliminated essentially all propulsive contractions from popliteal lymphatic vessels (Warthi *et al*., 2022; Davis *et al*., 2023d). Residual activity in some vessels was limited to small, localized diameter oscillations (<5 μm in amplitude) with irregular frequencies that were largely independent of pressure. As expected, the slope of the F-P relationship for *Cacna1c smKO* vessels was significantly reduced compared to $Cacna1c^{f/f}$ control vessels (Fig. 14B).

The T-type Ca^{2+} channel (Cav3.x) is critical for pacemaking in SA node (Lyashkov *et al*., 2018a), GI smooth muscle (Sanders, 2019) and renal pelvis smooth muscle (Grainger *et al*., 2022). Two Cav3 isoforms are expressed in LMCs: *Cacna1g* and *Cacna1h,* encoding Cav3.1 and Cav3.2 respectively (Lee *et al*., 2014; To *et al*., 2020). One report suggests that Cav3 channels are selectively involved in regulating the contraction frequency (but not amplitude) of rat mesenteric lymphatic collectors (Lee *et al*., 2014). We previously tested the roles of Cav3.1 and Cav3.2 in mouse lymphatic collectors and isolated LMCs after generating $Cacna1g^{-/-}$;$Cacna1h^{-/-}$ double KO mice (To *et al*., 2020). Here, we analyzed the slope of the F-P relationship in popliteal lymphatics from $Cacna1g^{-/-}$;$Cacna1h^{-/-}$ mice but found no significant differences from either WT or $Cav1.2^{f/f}$ control vessels (Fig. 14B), indicating that Cav3 channels are not involved in determining the F-P relationship.

Upstream pathways mediating pressure-induced chronotropy

Having established that ANO1, out of all the cation and K^+ channels tested, is the only current mediating pressure-induced lymphatic chronotropy, we then turned to an investigation of mechanosensitive pathways upstream from ANO1 channel activation.

Figure 12. Consequences of *Kcnq1* deletion.

UMAP and bubble plots of *Kcnq4* expression in the various IALV cell clusters. **B**) Slope of F-P relationship for popliteal lymphatics from WT *and Kcnq4 smKO* mice. **C**) Summary plots of contraction parameters as a function of pressure for the two respective groups of vessels. *Kcnq4 smKO* N=5, n=7.

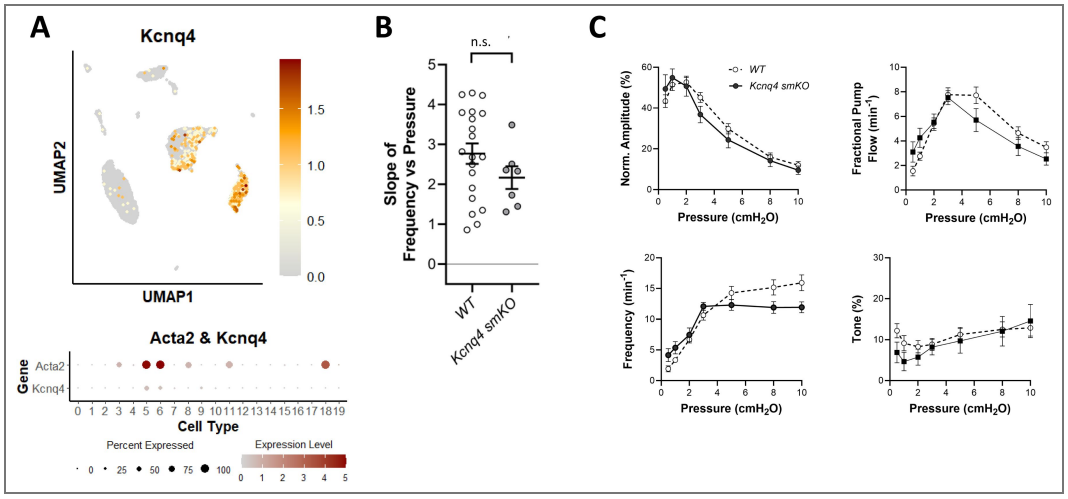

Figure 13. Consequences of Kir2.x inhibition.

UMAP and bubble plots of *Kcnj2* (Kir2.1*), Kcnj12 (*Kir2.2*)* and *Kcnj8* (*Kir6.1)* expression in various IALV cell clusters. **B**) Slope of F-P relationship for popliteal lymphatics from WT mice with/without treatment with the Kir2 inhibitor $BaCl_2$ (100 µM). WT N=15, n=20, WT+$BaCl_2$ N=4, n=11.

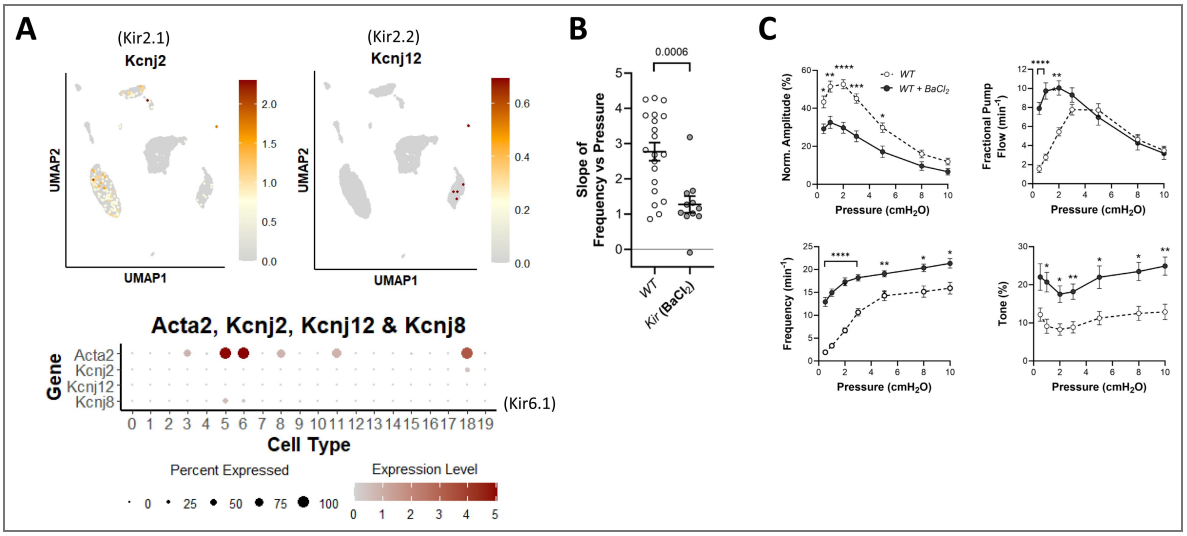

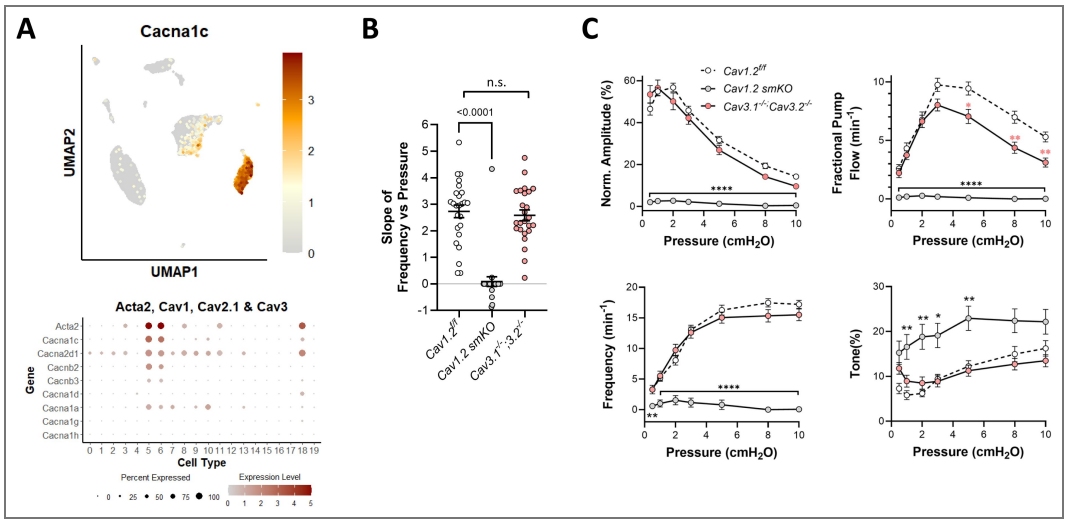

Figure 14. Consequences of *Cacna1c* (Cav1.2) and *Cacna1g/Cacna1h* (Cav3.1/3.2) deletion.

UMAP and bubble plots of the expression of voltage-gated Ca^{2+} channels and their accessory subunits in the various IALV cell clusters. **B**) Slope of F-P relationship for popliteal lymphatics from *Cacan1c*$^{f/f}$, *Cacna1c smKO* and *Cacna1g*$^{-/-}$;*Cacna1h*$^{-/-}$ mice. **C**) Summary plots of contraction parameters as a function of pressure for the three respective groups of vessels. *Cacna1c*: alpha-1c, *Cacna2d1*: α2/δ1, *Cacnb2*: β2, *Cacnb3*: β3, *Cacna1d*: alpha-1d ($Ca_V1.3$), *Cacna1a*: $Ca_V2.1$ (P/Q), *Cacna1g*: $Ca_V3.1$, *Cacna1h*: $Ca_V3.2$. *Cacna1c*$^{f/f}$ N=10, n=20; *Cacna1c smKO* N=14, n=24; *Cacna1g*$^{-/-}$;*Cacna1h*$^{-/-}$ N=16, n=25.

Role of IP_3R in pressure-induced chronotropy

Calcium release as a consequence of IP_3 generation is known to activate a number of ion channels and other proteins, including ANO1. We recently showed that genetic deletion of *Itpr1* (encoding IP_3R1) from mouse IALVs results in a reduction in spontaneous contraction frequency and a blunting of pressure-induced chronotropy similar to what is observed after *Ano1* deletion (Zawieja *et al*., 2023). scRNAseq analysis confirmed expression of *Itpr1* in >50% of LMCs (Fig. 15A). Here, we examined the consequences of *Itpr1* deletion in popliteal lymphatics by comparing the F-P relationship for vessels from Myh11-CreER^{T2};*Itpr1*$^{f/f}$ (*Itpr1 smKO*) and *Itpr1*$^{f/f}$mice. SM-specific deletion of *Itpr1* resulted in a significant reduction in the slope of the F-P relationship from 2.6 ± 0.3 to 0.6 ± 0.1 (Fig. 15B). Contraction data for *Itpr1 smKO* and *Itpr1*$^{f/f}$ control vessels are shown in Fig. 15C. The most striking features are 1) the significant reductions in frequency at all pressures and 2) a significant reduction in tone at elevated pressures in *Itpr1 smKO* vessels. The latter effect contrasts with the *increases* in tone observed after ANO1 inhibition or deletion (Fig. 2C). Collectively, these results show that IP_3R1 is critically important for pressure-induced lymphatic chronotropy in popliteal collecting vessels in much the same way it was previously documented in IALVs. Deletion of *Itpr1* in LMCs produces an effect on pressure-induced chronotropy similar to that of ANO1 deletion.

Role of GNAQ/GNA11 in pressure-induced chronotropy

Evidence from multiple studies specifically points to GNAQ/GNA11-coupled GPCRs as the upstream mechanosensing elements of myogenic constriction in arteries (Mederos y Schnitzler *et al*., 2008; Blodow *et al*., 2014; Harraz *et al*., 2014; Li *et al*., 2014b; Schleifenbaum *et al*., 2014; Pires *et al*., 2017; Bjorling *et al*., 2018). Mechanosensitive activation of one or more GPCRs independent of ligand binding (Zou *et al*., 2004; Erdogmus *et al*., 2019) could account for pressure-induced increases in IP_3 levels in LMCs. Our scRNAseq analysis revealed strong expression of *Gnaq* and *Gna11* in ~75% of LMCs, LECs, and AdvCs as well as very strong expression of *Gnaq* in some immune cell clusters (Fig. 16A). We tested the effects of SM-specific *Gnaq* knock out (Myh11-CreER^{T2};*Gnaq*$^{f/f}$), global *Gna11* knock out (*Gna11*$^{-/-}$) and *Gnaq*/*Gna11* double knock out (Myh11-CreER^{T2};*Gnaq*$^{f/f}$;*Gna11*$^{-/-}$) on pressure-induced lymphatic chronotropy. There was a trend for *Gnaq smKO* vessels to have a reduced slope in the F-P relationship in comparison to *Gnaq*$^{f/f}$;*Gna11*$^{+/+}$ control vessels, but it did not reach statistical significance (p=0.1296). However, global deletion of *Gna11* significantly reduced the slope of the F-P relationship and the reduction was even more significant and pronounced in *Gnaq*/*Gna11* double KO vessels (Fig. 16B). However, even combined knock out of both proteins did not cause an attenuation of pressure-induced chronotropy that was comparable to that observed after SM-specific *Itpr1* or *Ano1* deletion, particularly at pressures > 2 cmH_2O (compare Fig. 16B to Figs. 2B, 15B). Contraction data for *Gnaq smKO*, *Gna11*$^{-/-}$ and *Gna*$_q$/*Gna*$_{11}$double KO vessels, compared to tamoxifen-treated *Gnaq*$^{f/f}$;*Gna11*$^{+/+}$controls, are shown in Fig. 16C. The full F-P relationships for each genotype showed significant reductions in frequency at a few pressures for *Gnaq smKO* vessels compared to *Gnaq*$^{f/f}$;*Gna11*$^{+/+}$ controls, significant differences for *Gna11*$^{-/-}$ vessels at more pressures and significant differences at even more pressures for *Gnaq*/*Gna11* DKO vessels. Collectively, these results suggest that both GNAQ and GNA11-coupled G-proteins are involved in pressure-induced lymphatic chronotropy, with G11 being more important. However, the escape from inhibition at higher pressures points to the possible involvement of other mechanisms activating phospholipase(s) to generate IP_3.

Role of GNA12/GNA13 in pressure-induced chronotropy

Chennupati et al. (Chennupati *et al*., 2019) made the surprising finding that GNA12/GNA13-coupled GPCRs, rather than GNAQ/GNA11-coupled GPCRs, mediated myogenic constrictions in mesenteric and cerebral arteries of mice. GNA12/GNA13-coupled GPCRs are known to regulate contraction through Rho kinase (McDuffie *et al*., 2024) and one study of rat mesenteric lymphatics suggests that RhoK is essential for phasic lymphatic contractions (Kurtz *et al*., 2014). We investigated the effects of deleting both *Gna12* and *Gna13* from LMCs (Myh11-Cre^{T2};*Gna12*$^{f/f}$;*Gna13*$^{-/-}$ mice) on the F-P relationship of popliteal lymphatics. In the *Gna12*/*Gna13*

Figure 15. **Consequences of *Itpr1* (IP_3R1) deletion.**

UMAP and bubble plots of *Ip3r1* expression in the various IALV cell clusters. **B**) Slope of F-P relationship for popliteal lymphatics from *Itpr1*$^{f/f}$ *and Itpr1 smKO* mice. **C**) Summary plots of contraction parameters as a function of pressure for the two respective groups of vessels. *Itpr1 smKO* N=5, n=8; *Itpr1*$^{f/f}$ N=5, n=10.

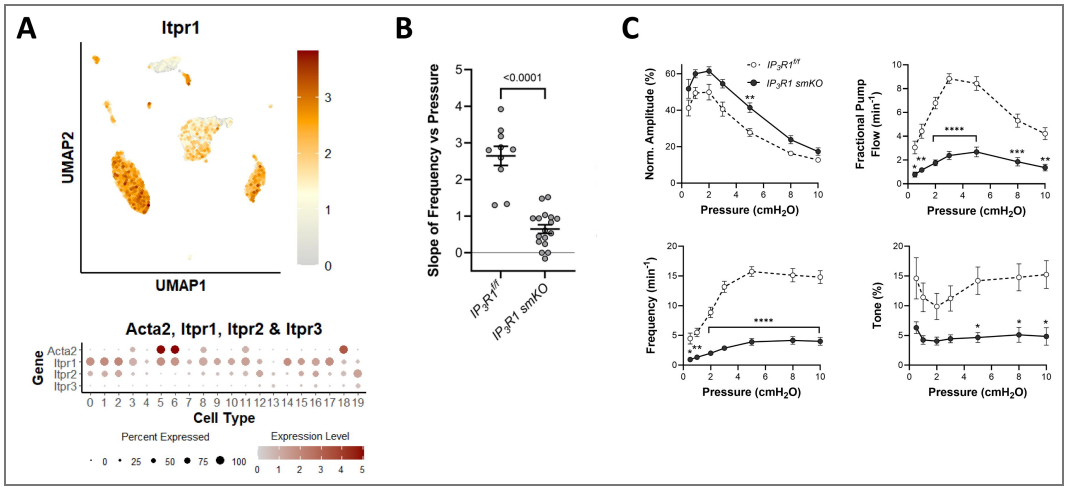

Figure 16. **Consequences of *Gnaq* and/or *Gna11* deletion.**

UMAP and bubble plots of *Gnaq* and *Gna11* expression in the various IALV cell clusters. **B**) Slope of F-P relationship for popliteal lymphatics from *Gnaq*$^{f/f}$;*Gna11*$^{+/+}$, Myh11-CreER^{T2};*Gnaq*$^{f/f}$ (Gnaq smKO*), Gna11*$^{-/-}$ *and* Myh11-CreER^{T2};*Gnaq*$^{f/f}$;*Gna11*$^{-/-}$ *DKO* mice. **C**) Summary plots of contraction parameters as a function of pressure for the four respective groups of vessels. *Gnaq*$^{f/f}$;*Gna11*$^{+/+}$ control N=3, n=6; *Gnaq smKO* N=4, n=8; *Gna11*$^{-/-}$ N=3, n=6; Myh11-CreER^{T2};*Gnaq*$^{f/f}$;*Gna11*$^{-/-}$N=8, n=13.

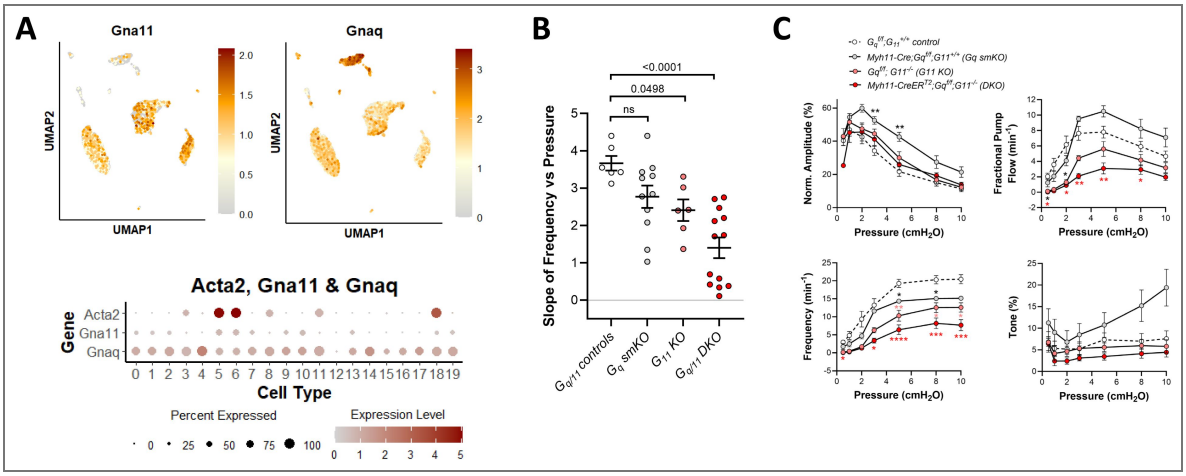

double knock out, contraction amplitude was significantly blunted and tone was significantly elevated at several pressures, but the F-P relationship was nearly identical to that of vessels from control *Gna12*$^{f/f}$;*Gna13*$^{+/+}$ mice (Fig. 17B-C).

Role of AT_1R in pressure-induced chronotropy

In many arteries, AT_1R is one of the predominantly expressed GPCRs and deletion of *Agtr1* results in loss or impairment of myogenic constriction in several types of arteries (Mederos y Schnitzler *et al*., 2008; Storch *et al*., 2012; Blodow *et al*., 2014; Schleifenbaum *et al*., 2014; Storch *et al*., 2015; Pires *et al*., 2017; Yamasaki *et al*., 2020). Selective deletion of the AT_1R isoform ($AT_{1a}R$ or $AT_{1b}R$) is sufficient to abrogate myogenic constriction in some arteries (Schleifenbaum *et al*., 2014; Pires *et al*., 2017). However, our scRNAseq analysis revealed almost no *Agtr1a* expression in LMCs, except in one possible subcluster (Fig. 18A). Pressure-induced chronotropy was measured in popliteal vessels from *Agtr1a*$^{-/-}$ mice and in vessels from WT mice treated with the AT_1R inhibitor losartan, which blocks both $AT_{1a}R$ and $AT_{1b}R$. We used a concentration of losartan (10 μM) known to be sufficient to block myogenic constriction in several types of arteries (Blodow *et al*., 2014; Jackson & Boerman, 2017; Yamasaki *et al*., 2020). However, neither inhibition of AT_1R nor deletion of *Agtr1a* impaired pressure-induced chronotropy, as evident by the absence of significant reductions in slope of the F-P relationship (Fig. 18B). Contraction data for these three groups are shown in Fig. 18C. Losartan treatment caused a slight impairment of contraction amplitude at several pressures but neither AT_1R blockade nor *Agtr1a* deletion significantly inhibited the F-P relationship, suggesting that AT_1R is not required for pressure-induced lymphatic chronotropy.

Discussion

Summary

The major goal of this study was to investigate the mechanistic basis of the F-P relationship in lymphatic muscle. The primary means by which lymphatic pumping is matched to excess filling of the interstitium is pressure-induced chronotropy—a >10-fold or more increase in contraction frequency with over the physiological pressure range (Davis *et al*., 2025). Because little was previously known regarding the mechanisms of mechanosensitivity underlying pressure-induced lymphatic chronotropy, we took cues from a well-studied mechanosensitive mechanism in vascular smooth muscle—the arterial myogenic response. In both arteries and collecting lymphatic vessels (Davis *et al*., 2009; Davis *et al*., 2023c), pressure elevation leads to vascular muscle cell depolarization and constriction, reflecting the activation of a depolarizing current that triggers Ca^{2+} entry through the opening of L-type, voltage-gated Ca^{2+} channels. Several ionic mechanisms have been previously implicated in this process for arterial smooth muscle, specifically the activation of TRPC6, TRPM4, PKD2, TRPV2 and ENaC cation channels (Welsh *et al*., 2002; Earley *et al*., 2004a; Jernigan & Drummond, 2005; Sharif-Naeini *et al*., 2009; McGahon *et al*., 2016), with supporting evidence for each obtained from gene knockdown / knockout studies. Additional ion channels may also be involved, including the activation of channels promoting Cl^- efflux (Boedtkjer *et al*., 2008) and the inhibition of constitutively active K^+ channels (Sancho *et al*., 2019), but evidence for those is based largely on the use of pharmacological inhibitors and therefore subject to concerns about off-target effects (Maroto *et al*., 2005; Dietrich *et al*., 2007; Gottlieb *et al*., 2008; Sancho *et al*., 2019). In the present study, we primarily used genetic knock out approaches to test the possible roles of the major ion channels contributing to the mechanosensitive chronotropy of lymphatic vessels from the mouse. Our results strongly support the conclusion that pressure-induced lymphatic chronotropy does *not* involve acute activation of any of the putative mechanosensitive (and/or second-messenger gated) cation channels previously implicated in myogenic constriction (TRPC6, TRPM4, PKD2, TRPV2, ENaC), nor does it require PIEZO1, the bona fide mechanosensitive cation channel implicated in other aspects of mechanotransduction in the cardiovascular system [see references in (Davis *et al*., 2023c)]. Rather, our results align with evidence from related studies of arterial smooth muscle showing that mechanotransduction of stretch/pressure is mediated by GNAQ/GNA11-coupled

Figure 17. Consequences of *Gna12*/*Gna13* deletion.

UMAP and bubble plots of *Gna12* and *Gna13* expression in the various IALV cell clusters. **B**) Slope of F-P relationship for popliteal lymphatics from *Gna12*$^{f/f}$;*Gna13*$^{+/+}$ *and* Myh11-CreER^{T2};*Gna12*$^{f/f}$;*Gna13*$^{-/-}$ *DKO* mice. **C**) Summary plots of contraction parameters as a function of pressure for the two respective groups of vessels. *Gna12*$^{f/f}$;*Gna13*$^{+/+}$ controls N=5, n=10; Myh11-CreER^{T2};*Gna12*$^{f/f}$;*Gna13*$^{-/-}$N=7, N=15.

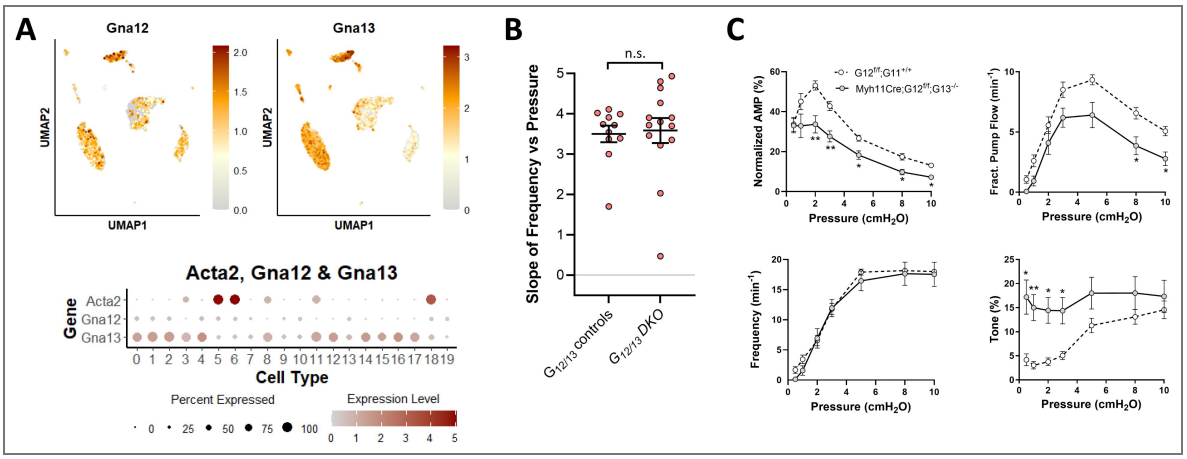

Figure 18. Consequences of *Agtr1* (AT_1R) deletion/inhibition.

UMAP and bubble plots of *Agtr1a* expression in the various IALV cell clusters. **B**) Slope of F-P relationship for popliteal lymphatics from WT mice with/without treatment with the AT_1R inhibitor losartan (10 μM) and *Agtr1a*$^{-/-}$ vessels. WT+losartan N=5, n=10; *Agtr1a*$^{-/-}$ N=3, n=6.

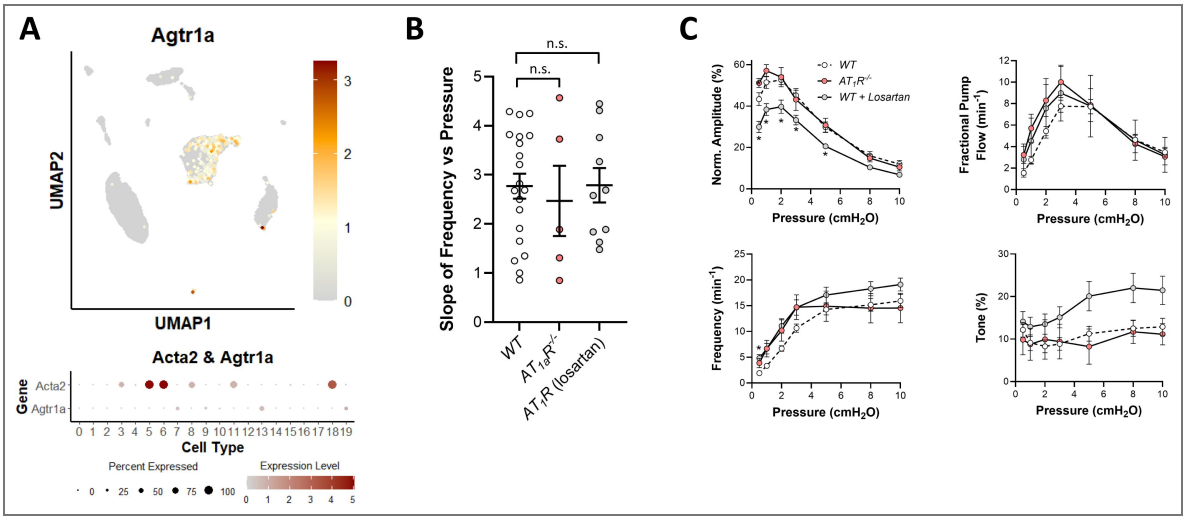

GPCRs, leading to downstream activation of second messenger-gated channels. In the case of LMCs, mechano-activation of GNAQ/GNA11-coupled GPCRs promotes IP_3 production that triggers Ca^{2+} release from stores through IP_3R1; Ca^{2+} then activates ANO1 Cl^- channels, which accelerate the rate of spontaneous diastolic depolarization, increasing the firing rate of action potentials that control phasic lymphatic contractions (Fig. 19). Repolarization is controlled in part by Kv channels (Cotton *et al*., 1997), including Kv11 channels (Kim *et al*., 2023). As summarized in Table 1, knockout of each element in the GNAQ/GNA11-IP_3-IP_3R1/Ca^{2+}-ANO1-Cav1.2 pathway (and only those elements out of all that were tested, except *Kcnj2/ Kcnj12*, which can be alternatively explained) abrogated or significantly attenuated pressure-induced chronotropy. Mechanosensitive regulation of ANO1 in this context is likely mediated by Ca^{2+} release from stores rather than possible direct (Ca^{2+}-independent) mechanosensitivity of ANO1 (Zou *et al*., 2025), because the similar degree of attenuation in the F-P relationship with *Iptr1* knockout as with *Ano1* smKO knock out shown here points to the involvement of an upstream mechanosensor.

Possible involvement of other G-coupled proteins

One inconsistency with the scheme suggested in Table 1 is that combined knock out of *Gnaq/Gna11* did not cause an attenuation of pressure-induced chronotropy comparable to that observed after SM-specific *Itpr1* or *Ano1* deletion, particularly at pressures > 2 cmH_2O (compare Fig. 16B to Figs. 2B, 15B). A possible explanation is that other G-coupled proteins are involved in mechanosensitive regulation of the GPCR-IP_3R1-Ca^{2+}-ANO1 signaling in LMCs. Indeed, two other G protein-coupled effectors, *Gna14* and *Gna15* in the GNAQ family, could also be activated downstream of pressure-induced GPCR activation and potentially mediate IP_3/DAG production. We have included *Gna14* (*Gna14* is expressed in 28% of LMCs in our dataset) in the summary scheme shown in Fig. 19 but its role in IP_3 production and ANO1 activation remains to be investigated. Even so, inclusion of other G protein-coupled effectors would still fail to account for the residual pacemaking observed after apparently complete deletion of ANO1. We use the phrase “apparently complete” because incomplete recombination by the inducible Myh11-$CreER^{T2}$ remains a possibility. Although we could not detect residual message for *Ano1* in Myh11-$CreER^{T2}$;$Ano1^{f/f}$ mice after tamoxifen treatment (Fig. 3B), that message was measured in LMCs digested from IALVs inguinal-axillary lymphatic vessels (chosen because of a higher cell yield), whereas the F-P relationship was measured in popliteal lymphatic vessels (chosen because of the greater dynamic range in F-P).

We also investigated the possible role of GNA12/GNA13-coupled GPCRs in the F-P relationship, based on a study showing that GNA12/GNA13, rather than GNAQ/GNA11, is required for myogenic constriction in arterial smooth muscle (Chennupati *et al*., 2019) and a paper showing that RhoK (known to be activated downstream from GNA12/GNA13 activation) is critical for phasic lymphatic contractions and associated phasic LMC Ca^{2+} signaling (Kurtz *et al*., 2014). However, *Gna12/Gna13* double knock out resulted in no significant change in the F-P slope (Fig. 17B), and there were no differences in frequency at any pressure compared to $Gna12^{f/f}$; $Gna13^{+/+}$ control vessels (Fig. 17C).

Roles for ion channels in other aspects of LMC contractile function

Originally, we hypothesized that an ion channel (other than ANO1) was involved in LMC pacemaking. If IP_3 production in LMCs is enhanced after pressure elevation, as it is in arterial smooth muscle (Narayanan *et al*., 1994; Mederos y Schnitzler *et al*., 2008), then concomitant increases in DAG, the other product of PIP_2 hydrolysis, would also be predicted to occur, and DAG should then activate TRP6C and related channels. However, if this occurs in popliteal lymphatic vessels, the activation of those channels apparently does not significantly influence the F-P relationship (Fig. 4). Likewise, the Ca^{2+} increase resulting from mechanosensitive activation of the GNAQ/GNA11-IP_3-IP_3R1 signaling axis would potentially activate TRPM4 and/or PKD2 (assuming those channels are localized to the appropriate LMC microdomains), but we find that their deletion does not alter the F-P relationship (Figs. 5-6). Because TRPM4, PKD2 and PIEZO1 expression levels are very low in LMCs (Figs. 3A,4A, 5A), further activation of those

Figure 19. Proposed mechanotransduction mechanism underlying pressure-induced chronotropy.

Summary diagram depicting the primary signaling pathway through which changes in pressure regulate the frequency of the ionic pacemaker. GNAQ/GNA11-coupled GPCRs are the primary, but not exclusive mechanosensor. ANO1 is the primary, but not exclusive effector. Kv11 provides at least one source of repolarizing signal (Kim *et al*., 2023).

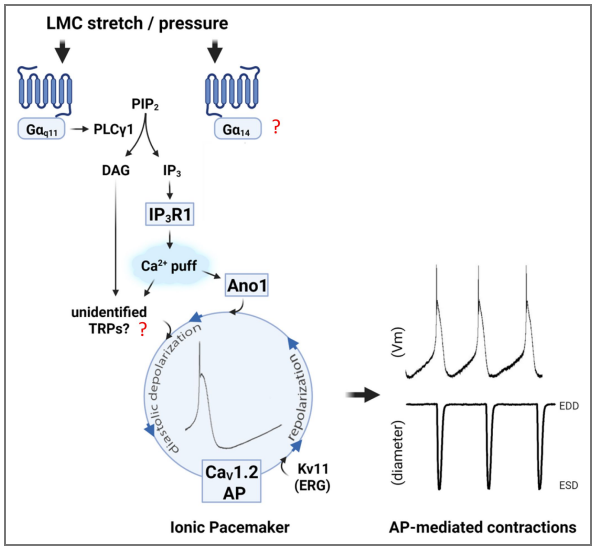

Table 1. Genes for which deletion/inhibition produced significant attenuation or enhancement of the F-P relationship.

Attenuation	Enhancement
Cacna1c	*TrpC6/TrpC3*
Ano1	-
Itpr1	-
Gnaq	-
Gna11	-
Kcnj2/Kcnj12	-

channels may have little effect. It is possible that another unidentified ion channel could be mediating the pressure-driven frequency changes at higher pressures—perhaps a channel with a higher mechanosensitive threshold or requiring higher levels of IP_3, DAG or Ca^{2+}. Candidates include TRPV1, which has also been implicated in arterial myogenic constriction (Phan *et al*., 2022).

Although the deletion/inhibition of several TRP channel family members and other channels did not significantly impact pressure-induced chronotropy, it did impact other aspects of lymphatic contractile function, namely contraction amplitude and/or tone. The respective channels and their statistically significant contraction effects are summarized in Table 2. Deletion of TRPC6/TRPC3 impaired contraction amplitude by ~40% and increased tone by ~2.5-fold (Fig. 4C). Deletion of TRPV4 from LMCs impaired contraction amplitude by ~45% without an effect on tone (Fig. 7C). TRPV4 channel activation has recently been implicated in the regulation of lymphatic contraction, but primarily via the production of vasoactive products from LECs and resident macrophages (Schulz *et al*., 2025). There were three other channels whose inhibition led to significant changes in amplitude and/or tone. Specifically, one of the two TRPV2 inhibitors (SET2) inhibited tone at 4 of the 5 lowest pressures. One of the two ENaC inhibitors (amiloride) inhibited amplitude by 20-30% while the other one (benzamil) enhanced tone by ~2-fold (Fig. 9C). The Kir2 blocker Ba^{2+} impaired amplitude by ~40% and increased tone by 2-fold (Fig. 13C). Collectively, these effects suggest that the respective channels are each involved in some aspect of lymphatic contractile function (other than pressure-induced chronotropy), with the more compelling evidence being that obtained after by gene deletion rather than after acute application of soluble inhibitors, which may have off-target effects.

Future directions

Lastly, the critical mechanosensitive GNAQ/GNA11-coupled GPCR(s) in LMCs remain(s) to be identified. Although evidence points to AT_1R as the key GNAQ/GNA11 –coupled mechanosensitive GPCR in arterial smooth muscle (Mederos y Schnitzler *et al*., 2011; Davis *et al*., 2023c), message for AT_1R is negligible in LMCs (Fig. 18A) and neither *Agtr1* knock out or pharmacologic AT_1R blockade altered pressure-induced chronotropy (Fig. 18B-C). No studies to date have attempted to identify the major GPCRs expressed in LMCs, e.g., by analyzing the various published scRNAseq databases for LMCs (Kenney *et al*., 2022; Lei *et al*., 2025; Schulz *et al*., 2025; Zawieja *et al*., 2025), but doing so might provide a starting point for identifying the specific mechanosensitive GNAQ/GNA11 - coupled (and other) GPCRs that mediate pressure-induced chronotropy.

Physiological Relevance

LMC function is impaired in Cantú syndrome, the only known example of primary lymphedema produced by a gene mutation (*Kcnj8/Abbc9*) in LMCs (Davis *et al*., 2023b). This impairment is evident both in lower contraction frequencies and amplitudes at multiple pressure levels. The lower frequency is consistent with parallel observations that gain-of-function mutations in K_{ATP} channels increase metabolic stress (Kim *et al*., 2024), whereas the lower amplitude suggests that other aspects of LMC function are altered as a consequence of chronic K_{ATP} channel hyperactivation. It is interesting that lymphatic contraction frequency and amplitude are also impaired in secondary lymphedema, in aging and in various models of metabolic disease [(Castorena-Gonzalez *et al*., 2025) and see discussion and references in (Davis *et al*., 2023e)]. Potential therapies for reversing LMC dysfunction under these conditions will depend on identifying the key ion channels and signaling pathways that drive pacemaking and control contraction amplitude. The present study represents a major step forward in the identification of specific LMC targets that could be used for that purpose.

Acknowledgements

The authors are grateful for the technical assistance of Shanyu Ho. We acknowledge the kind gifts of *Kcnq4*$^{-/-}$ mice from Thomas Jentsch (Free University of Berlin), *Trpc6*$^{-/-}$ and *Trpc3*$^{-/-}$ mice from Lutz Birnbaumer (NIH), *Piezo1*$^{f/f}$ mice from Ardem Patapoutian (USCD), and *Itpr1*$^{f/f}$ mice from Ju

Table 2. **Consequences of deletion/inhibition of ion channels on contraction amplitude and/or tone.***

Channel	Effect on AMP	Effect on Tone	Method of inhibition
TRPC6/3	↓	↓	deletion
TRPV4	↓	-	deletion
TRPV2	-	↓	soluble inhibitor
ENaC	↓	↑	soluble inhibitor
Kir2.x	↓	↑	soluble inhibitor

* Excluding the GNAQ/GNA11-IP_3R1/Ca^{2+}-ANO1-Cav1.2 signaling pathway.

Suppl. Table 1. **Primers used for qPCR.**

Gene	Accession Number	Catalog Number	Description
Ano1	NM_178642	IDT Mm.PT.58.12522115	Mouse Ano1 TaqMan probe
Acta2	NM_007392	IDT Mm.PT.58.16320644	Mouse α-actin TaqMan probe
β-Actin	NM_007393	IDT Mm.PT.58.33257376.gs	Mouse Actb TaqMan probe

Chen (UCSD). *Ano1*$^{f/f}$ and Myh11-CreER^{T2};*Pkd2*$^{f/f}$ mice were gifts from Jonathan Jaggar (University of Tennessee HSC). Stefan Offermanns (Max-Planck-Institute, Bad Nauheim) kindly provided sperm from *Gna*$_{12}^{-/-}$;*Gna*$^{f/f}$ and *Gna*$^{-/-}$;*Gna*$^{f/f}$ mice. This work was supported by National Institutes of Health grants (R01-HL122578 to MJD; R01-HL168568 to JAC-G; R35-HL155008 to SE; R01-HL136292 to TLD; R01-HL142905 to JPS; R01-HL143198 to SDZ).

Additional information

Data availability

RNA sequence data were deposited in GEO (accession number GSE277843). All data generated or analyzed during this study are included in the manuscript and supporting files; source data files have been provided for all figures.

Author Contributions

MJD and SDZ designed the experiments. MJD, JAC-G, ML, SDZ and JK performed the experiments and analyzed the results. ML bred, managed and genotyped the mouse lines. TLD and SE generated and provided mouse lines. MJD drafted the manuscript. All authors edited the manuscript and approved the final version.

Funding

Funder	Grant reference number	Author
National Institutes of Health	R01-HL122578	Michael J Davis
National Institutes of Health	R01-HL168568	Jorge A Castorena-Gonzalez
National Institutes of Health	R35-HL155008	Scott Earley
National Institutes of Health	R01-HL136292	Timothy Domeier
National Institutes of Health	R01-HL143198	Scott D Zawieja
National Institutes of Health	R01-HL142905	Joshua Scallan

Author ORCID iDs

Michael J Davis: http://orcid.org/0000-0002-7992-9300

References

Accili EA, Proenza C, Baruscotti M, DiFrancesco D (2002) From funny current to HCN channels: 20 years of excitation. *News in Physiological Science* **17**:32-37

Ahn SJ, Fancher IS, Bian JT, Zhang CX, Schwab S, Gaffin R, Phillips SA, Levitan I (2017) Inwardly rectifying K(+) channels are major contributors to flow-induced vasodilatation in resistance arteries. *J Physiol* **595**:2339-2364

Alotaibi M, Kahlat K, Nedjadi T, Djouhri L (2017) Effects of ZD7288, a hyperpolarization-activated cyclic nucleotide-gated (HCN) channel blocker, on term-pregnant rat uterine contractility in vitro. *Theriogenology* **90**:141-146

Benos DJ (2004) Sensing tension: recognizing ENaC as a stretch sensor. *Hypertension* **44**:616-617

Bjorling K, Joseph PD, Egebjerg K, Salomonsson M, Hansen JL, Ludvigsen TP, Jensen LJ (2018) Role of age, Rho-kinase 2 expression, and G protein-mediated signaling in the myogenic response in mouse small mesenteric arteries. *Physiol Rep* **6**:e13863

Blodow S, Schneider H, Storch U, Wizemann R, Forst AL, Gudermann T, Mederos y Schnitzler M. (2014) Novel role of mechanosensitive AT1B receptors in myogenic vasoconstriction. *Pflugers Arch* **466**:1343-1353

Boedtkjer DM, Matchkov VV, Boedtkjer E, Nilsson H, Aalkjaer C (2008) Vasomotion has chloride-dependency in rat mesenteric small arteries. *Pflugers Arch* **457**:389-404

Bogdanov KY, Vinogradova TM, Lakatta EG (2001) Sinoatrial nodal cell ryanodine receptor and Na(+)-Ca(2+) exchanger: molecular partners in pacemaker regulation. *Circ Res* **88**:1254-1258

Bulley S, Fernandez-Pena C, Hasan R, Leo MD, Muralidharan P, Mackay CE, Evanson KW, Moreira-Junior L, Mata-Daboin A, Burris SK, *et al.* (2018) Arterial smooth muscle cell PKD2 (TRPP1) channels regulate systemic blood pressure. *eLife* **7**

Castorena-Gonzalez JA, Kim HJ, Davis MJ (2025) Chronic metabolic stress impairs lymphatic contractility via activation of KATP channels in a mouse model of Type-2 diabetes. *Front Physiol* **16**:1558763

Chen YL, Sonkusare SK (2020) Endothelial TRPV4 channels and vasodilator reactivity. *Curr Top Membr* **85**:89-117

Chennupati R, Wirth A, Favre J, Li R, Bonnavion R, Jin YJ, Wietelmann A, Schweda F, Wettschureck N, Henrion D, *et al.* (2019) Myogenic vasoconstriction requires G12/G13 and LARG to maintain local and systemic vascular resistance. *eLife* **8**

Choi D, Park E, Choi J, Lu R, Yu JS, Kim C, Zhao L, Yu J, Nakashima B, Lee S, *et al.* (2024) Piezo1 regulates meningeal lymphatic vessel drainage and alleviates excessive CSF accumulation. *Nat Neurosci*

Choi D, Park E, Jung E, Cha B, Lee S, Yu J, Kim PM, Lee S, Hong YJ, Koh CJ, *et al.* (2019) Piezo1 incorporates mechanical force signals to genetic program that governs lymphatic valve development and maintenance. *JCI Insight*

Coste B, Mathur J, Schmidt M, Earley TJ, Ranade S, Petrus MJ, Dubin AE, Patapoutian A (2010) Piezo1 and Piezo2 are essential components of distinct mechanically activated cation channels. *Science* **330**:55-60

Cotton KD, Hollywood MA, McHale NG, Thorbury KD (1997) Outward currents in smooth muscle cells isolated from sheep mesenteric lymphatics. *Journal of Physiology* **503**:1-11

Davis MJ (2005) An improved, computer-based method to automatically track internal and external diameter of isolated microvessels. *Microcirculation* **12**:361-372

Davis MJ (2012) Physiological role(s) of the vascular myogenic response. *Microcirculation* **19**:99-114

Davis MJ (2023a) Diameter tracking program for quantitative assessment of lymphatic vessel contractions. Zenodo. https://doi.org/10.5281/zenodo.8286119

Davis MJ (2023b) Pressure acquisition and control program for quantitative assessment of lymphatic vessel function. Zenodo. https://doi.org/10.5281/zenodo.8286107

Davis MJ, Castorena-Gonzalez J, Zawieja SD (2023a) Electric field stimulation unmasks a subtle role for T-type calcium channels in regulating lymphatic contraction. *Scientific Reports* **13**:15862

Davis MJ, Castorena-Gonzalez JA, Kim HJ, Li M, Remedi M, Nichols CG. (2023b) Lymphatic contractile dysfunction in mouse models of Cantu Syndrome with K(ATP) channel gain-of-function. *Function (Oxf)* **4**:zqad017

Davis MJ, Davis AM, Ku CW, Gashev AA (2009) Myogenic constriction and dilation of isolated lymphatic vessels. *American Journal of Physiology (Heart and Circulatory Physiology)* **296**:H293-H302

Davis MJ, Earley S, Li YS, Chien S (2023c) Vascular mechanotransduction. *Physiol Rev* **103**:1247-1421

Davis MJ, Kim HJ, Li M, Zawieja SD (2023d) A vascular smooth muscle-specific integrin alpha8 Cre mouse for lymphatic contraction studies that allows male-female comparisons and avoids lethal visceral myopathy. *Frontiers in Physiology* **13**:1060146

Davis MJ, Kim HJ, Zawieja SD, Castorena-Gonzalez JA, Gui P, Li M, Saunders BT, Zinselmeyer BH, Randolph GJ, Remedi MS, *et al.* (2020) Kir6.1-dependent K(ATP) channels in lymphatic smooth muscle and vessel dysfunction in mice with Kir6.1 gain-of-function. *J Physiol* **598**:3107-3127

Davis MJ, King PD, Zawieja SD (2025) Transport and immune functions of the lymphatic system. *Annual Review of Physiology* **87**:151-172

Davis MJ, Scallan JP, Castorena-Gonzalez JA, Kim HJ, Ying LH, Pin YK, Angeli V (2023e) Multiple aspects of lymphatic dysfunction in an ApoE (-/-) mouse model of hypercholesterolemia. *Front Physiol* **13**:1098408

Davis MJ, Scallan JP, Wolpers JH, Muthuchamy M, Gashev AA, Zawieja DC (2012) Intrinsic increase in lymphangion muscle contractility in response to elevated afterload. *Am J Physiol Heart Circ Physiol* **303**:H795-H808

Davis MJ, Zawieja SD. (2018) Electrical pacemaking in lymphatic vessels. In: Earley S, Trebak M (Eds). *Signal Transduction and Smooth Muscle* Boca Raton: CRC Press. pp. 323-359

Davis MJ, Zawieja SD (2024) Pacemaking in the lymphatic system. *Journal of Physiology*

Dietrich A, Kalwa H, Storch U, Mederos y Schnitzler M, Salanova B, Pinkenburg O, Dubrovska G, Essin K, Gollasch M, Birnbaumer L, *et al.* (2007) Pressure-induced and store-operated cation influx in vascular smooth muscle cells is independent of TRPC1. *Pflugers Arch* **455**:465-477

Dietrich A, Mederos YSM, Gollasch M, Gross V, Storch U, Dubrovska G, Obst M, Yildirim E, Salanova B, Kalwa H, *et al.* (2005) Increased vascular smooth muscle contractility in TRPC6-/- mice. *Mol Cell Biol* **25**:6980-6989

Drummond HA (2012) betaENaC is a molecular component of a VSMC mechanotransducer that contributes to renal blood flow regulation, protection from renal injury, and hypertension. *Front Physiol* **3**:341

Earley S, Brayden JE (2015) Transient receptor potential channels in the vasculature. *Physiol Rev* **95**:645-690

Earley S, Waldron BJ, Brayden JE (2004a) Critical role for transient receptor potential channel TRPM4 in myogenic constriction of cerebral arteries. *Circulation Research* **95**:922-929

Earley S, Waldron BJ, Brayden JE (2004b) Critical role for transient receptor potential channel TRPM4 in myogenic constriction of cerebral arteries. *Circ Res* **95**:922-929

Erdogmus S, Storch U, Danner L, Becker J, Winter M, Ziegler N, Wirth A, Offermanns S, Hoffmann C, Gudermann T, *et al.* (2019) Helix 8 is the essential structural motif of mechanosensitive GPCRs. *Nat Commun* **10**:5784

Germain PL, Lun A, Garcia Meixide C, Macnair W, Robinson MD (2021) Doublet identification in single-cell sequencing data using scDblFinder. *F1000Res* **10**:979

Gonzales AL, Earley S (2013) Regulation of cerebral artery smooth muscle membrane potential by Ca(2)(+)-activated cation channels. *Microcirculation* **20**:337-347

Gonzales AL, Yang Y, Sullivan MN, Sanders L, Dabertrand F, Hill-Eubanks DC, Nelson MT, Earley S (2014) A PLCgamma1-dependent, force-sensitive signaling network in the myogenic constriction of cerebral arteries. *Sci Signal* **7**:ra49

Gottlieb P, Folgering J, Maroto R, Raso A, Wood TG, Kurosky A, Bowman C, Bichet D, Patel A, Sachs F, *et al.* (2008) Revisiting TRPC1 and TRPC6 mechanosensitivity. *Pflugers Arch* **455**:1097-1103

Grainger N, Shonnard CC, Quiggle SK, Fox EB, Presley H, Daugherty R, Shonnard MC, Drumm BT, Sanders KM. (2022) Propagation of Pacemaker Activity and Peristaltic Contractions in the Mouse Renal Pelvis Rely on Ca(2+)-activated Cl(-) Channels and T-Type Ca(2+) Channels. *Function (Oxf)* **3**:zqac041

Hao Y, Hao S, Andersen-Nissen E, Mauck WM, Zheng S, Butler A, Lee MJ, Wilk AJ, Darby C, Zager M, *et al.* (2021) Integrated analysis of multimodal single-cell data. *Cell* **184**:3573-3587.

Hao Y, Stuart T, Kowalski MH, Choudhary S, Hoffman P, Hartman A, Srivastava A, Molla G, Madad S, Fernandez-Granda C, *et al.* (2024) Dictionary learning for integrative, multimodal and scalable single-cell analysis. *Nat Biotechnol* **42**:293-304

Harder DR (1984) Pressure-dependent membrane depolarization in cat middle cerebral artery. *Circulation Research* **55**:197-202

Harraz OF, Abd El-Rahman RR, Bigdely-Shamloo K, Wilson SM, Brett SE, Romero M, Gonzales AL, Earley S, Vigmond EJ, Nygren A, *et al.* (2014) Ca(V)3.2 channels and the induction of negative feedback in cerebral arteries. *Circ Res* **115**:650-661

Hwang SJ, Basma N, Sanders KM, Ward SM (2016) Effects of new-generation inhibitors of the calcium-activated chloride channel anoctamin 1 on slow waves in the gastrointestinal tract. *Br J Pharmacol* **173**:1339-1349

Jackson WF, Boerman EM (2017) Regional heterogeneity in the mechanisms of myogenic tone in hamster arterioles. *Am J Physiol Heart Circ Physiol* **313**:H667-H675

Jernigan NL, Drummond HA (2005) Vascular ENaC proteins are required for renal myogenic constriction. *American Journal of Physiology (Renal Physiology)* **289**:F891-F901

Jernigan NL, Drummond HA (2006) Myogenic vasoconstriction in mouse renal interlobar arteries: role of endogenous beta and gammaENaC. *American Journal of Physiology (Renal Physiology)* **291**:F1184-F1191

Kenney HM, Wu CL, Loiselle AE, Xing L, Ritchlin CT, Schwarz EM (2022) Single-cell transcriptomics of popliteal lymphatic vessels and peripheral veins reveals altered lymphatic muscle and immune cell populations in the TNF-Tg arthritis model. *Arthritis Res Ther* **24**:64

Kim HJ, Li M, Erlich EC, Randolph GJ, Davis MJ (2023) ERG K(+) channels mediate a major component of action potential repolarization in lymphatic muscle. *Sci Rep* **13**:14890

Kim HJ, Norton CE, Zawieja SD, Castorena-Gonzalez JA, Davis MJ. (2024) Acute Metabolic Stress Induces Lymphatic Dysfunction Through KATP Channel Activation. *Function* **5**:zqae033

Kurtz KH, Souza-Smith FM, Moor AN, Breslin JW (2014) Rho kinase enhances contractions of rat mesenteric collecting lymphatics. *PLoS One* **9**:e94082

Lee S, Roizes S, von der Weid PY. (2014) Distinct roles of L- and T-type voltage-dependent Ca2+ channels in regulation of lymphatic vessel contractile activity. *Journal of Physiology* **592**:5409-5427

Lei PJ, Ruscic KJ, Roh K, Rajotte JJ, O'Melia MJ, Bouta EM, Marquez M, Pereira ER, Kumar AS, Razavi MS, *et al.* (2025) Aging-induced changes in lymphatic muscle cell transcriptomes are associated with reduced pumping of peripheral collecting lymphatic vessels in mice. *Dev Cell* **60**:1118-1133.

Levick JR, Michel CC (2010) Microvascular fluid exchange and the revised Starling principle. *Cardiovascular Research* **87**:198-210

Li H, Wei H, Padera TP, Baish JW, Munn LL. (2022) Computational simulations of the effects of gravity on lymphatic transport. *PNAS Nexus* **1**:pgac237

Li J, Hou B, Tumova S, Muraki K, Bruns A, Ludlow MJ, Sedo A, Hyman AJ, McKeown L, Young RS, *et al.* (2014a) Piezo1 integration of vascular architecture with physiological force. *Nature* **515**:279-282

Li Y, Baylie RL, Tavares MJ, Brayden JE (2014b) TRPM4 channels couple purinergic receptor mechanoactivation and myogenic tone development in cerebral parenchymal arterioles. *J Cereb Blood Flow Metab* **34**:1706-1714

Longden TA, Dabertrand F, Koide M, Gonzales AL, Tykocki NR, Brayden JE, Hill-Eubanks D, Nelson MT (2017) Capillary K(+)-sensing initiates retrograde hyperpolarization to increase local cerebral blood flow. *Nat Neurosci* **20**:717-726

Lyashkov AE, Behar J, Lakatta EG, Yaniv Y, Maltsev VA (2018a) Positive Feedback Mechanisms among Local Ca Releases, NCX, and I(CaL) Ignite Pacemaker Action Potentials. *Biophys J* **114**:1176-1189

Lyashkov AE, Behar J, Lakatta EG, Yaniv Y, Maltsev VA (2018b) Positive Feedback Mechanisms among Local Ca Releases, NCX, and ICaL Ignite Pacemaker Action Potentials. *Biophys J* **114**:2024

Mader F, Muller S, Krause L, Springer A, Kernig K, Protzel C, Porath K, Rackow S, Wittstock T, Frank M, *et al.* (2018) Hyperpolarization-Activated Cyclic Nucleotide-Gated Non-selective (HCN) Ion Channels Regulate Human and Murine Urinary Bladder Contractility. *Front Physiol* **9**:753

Majgaard J, Skov FG, Kim S, Hjortdal VE, Boedtkjer DMB (2022) Positive chronotropic action of HCN channel antagonism in human collecting lymphatic vessels. *Physiol Rep* **10**:e15401

Mani BK, Byron KL (2011) Vascular KCNQ channels in humans: the sub-threshold brake that regulates vascular tone?. *Br J Pharmacol* **162**:38-41

Maroto R, Raso A, Wood TG, Kurosky A, Martinac B, Hamill OP (2005) TRPC1 forms the stretch-activated cation channel in vertebrate cells. *Nature Cell Biology* **7**:179-185

Mathar I, Vennekens R, Meissner M, Kees F, Van der Mieren G, Camacho Londono JE, Uhl S, Voets T, Hummel B, van den Bergh A, *et al.* (2010) Increased catecholamine secretion contributes to hypertension in TRPM4-deficient mice. *Journal of Clinical Investigation* **120**:3267-3279

McDuffie EL, Panettieri RA, Scott CP (2024) G(12/13) signaling in asthma. *Respir Res* **25**:295

McGahon MK, Fernandez JA, Dash DP, McKee J, Simpson DA, Zholos AV, McGeown JG, Curtis TM. (2016) TRPV2 Channels Contribute to Stretch-Activated Cation Currents and Myogenic Constriction in Retinal Arterioles. *Invest Ophthalmol Vis Sci* **57**:5637-5647

Mederos y Schnitzler M, Storch U, Gudermann T. (2011) AT1 receptors as mechanosensors. *Curr Opin Pharmacol* **11**:112-116

Mederos y Schnitzler M, Storch U, Meibers S, Nurwakagari P, Breit A, Essin K, Gollasch M, Gudermann T. (2008) Gq-coupled receptors as mechanosensors mediating myogenic vasoconstriction. *EMBO J* **27**:3092-3103

Mercado J, Baylie R, Navedo MF, Yuan C, Scott JD, Nelson MT, Brayden JE, Santana LF (2014) Local control of TRPV4 channels by AKAP150-targeted PKC in arterial smooth muscle. *J Gen Physiol* **143**:559-575

Monfredi O, Maltseva LA, Spurgeon HA, Boyett MR, Lakatta EG, Maltsev VA (2013) Beat-to-Beat Variation in Periodicity of Local Calcium Releases Contributes to Intrinsic Variations of Spontaneous Cycle Length in Isolated Single Sinoatrial Node Cells. *PLoS One* **8**:e67247

Muraki K, Iwata Y, Katanosaka Y, Ito T, Ohya S, Shigekawa M, Imaizumi Y (2003) TRPV2 is a component of osmotically sensitive cation channels in murine aortic myocytes. *Circ Res* **93**:829-838

Murthy SE, Dubin AE, Patapoutian A (2017) Piezos thrive under pressure: mechanically activated ion channels in health and disease. *Nat Rev Mol Cell Biol* **18**:771-783

Narayanan D, Bulley S, Leo MD, Burris SK, Gabrick KS, Boop FA, Jaggar JH (2013) Smooth muscle cell transient receptor potential polycystin-2 (TRPP2) channels contribute to the myogenic response in cerebral arteries. *J Physiol* **591**:5031-5046

Narayanan J, Imig M, Roman RJ, Harder DR (1994) Pressurization of isolated renal arteries increases inositol trisphosphate and diacylglycerol. *American Journal of Physiology (Heart and Circulatory Physiology)* **266**:H1840-H1845

Negrini D, Marcozzi C, Solari E, Bossi E, Cinquetti R, Reguzzoni M, Moriondo A (2016) Hyperpolarization-activated cyclic nucleotide-gated channels in peripheral diaphragmatic lymphatics. *Am J Physiol Heart Circ Physiol* **311**:H892-H903

Nilius B, Droogmans G (2001) Ion channels and their functional role in vascular endothelium. *Physiological Reviews* **81**:1415-1459

Nonomura K, Lukacs V, Sweet DT, Goddard LM, Kanie A, Whitwam T, Ranade SS, Fujimori T, Kahn ML, Patapoutian A (2018) Mechanically activated ion channel PIEZO1 is required for lymphatic valve formation. *Proc Natl Acad Sci U S A* **115**:12817-12822

Olszewski WL, Engeset A (1980) Intrinsic contractility of prenodal lymph vessels and lymph flow in human leg. *American Journal of Physiology (Heart and Circulatory Physiology)* **239**:H775-H783

Peyronnet R, Martins JR, Duprat F, Demolombe S, Arhatte M, Jodar M, Tauc M, Duranton C, Paulais M, Teulon J, *et al.* (2013) Piezo1-dependent stretch-activated channels are inhibited by Polycystin-2 in renal tubular epithelial cells. *EMBO Rep* **14**:1143-1148

Phan TX, Ton HT, Gulyas H, Porszasz R, Toth A, Russo R, Kay MW, Sahibzada N, Ahern GP (2022) TRPV1 in arteries enables a rapid myogenic tone. *J Physiol* **600**:1651-1666

Pires PW, Ko EA, Pritchard HAT, Rudokas M, Yamasaki E, Earley S (2017) The angiotensin II receptor type 1b is the primary sensor of intraluminal pressure in cerebral artery smooth muscle cells. *J Physiol* **595**:4735-4753

Price MP, Lewin GR, McIlwrath SL, Cheng C, Xie J, Heppenstall PA, Stucky CL, Mannsfeldt AG, Brennan TJ, Drummond HA, *et al.* (2000) The mammalian sodium channel BNC1 is required for normal touch sensation. *Nature* **407**:1007-1011

Renkin EM (1986) Some consequences of capillary permeability to macromolecules: Starling's hypothesis reconsidered. *Am J Physiol* **250**:H706-710

Retailleau K, Duprat F, Arhatte M, Ranade SS, Peyronnet R, Martins JR, Jodar M, Moro C, Offermanns S, Feng Y, *et al.* (2015) Piezo1 in Smooth Muscle Cells Is Involved in Hypertension-Dependent Arterial Remodeling. *Cell Rep* **13**:1161-1171

Sancho M, Fabris S, Hald BO, Brett SE, Sandow SL, Poepping TL, Welsh DG (2019) Membrane Lipid-KIR2.x Channel Interactions Enable Hemodynamic Sensing in Cerebral Arteries. *Arterioscler Thromb Vasc Biol* **39**:1072-1087

Sancho M, Samson NC, Hald BO, Hashad AM, Marrelli SP, Brett SE, Welsh DG (2017) KIR channels tune electrical communication in cerebral arteries. *J Cereb Blood Flow Metab* **37**:2171-2184

Sanders KM (2019) Spontaneous Electrical Activity and Rhythmicity in Gastrointestinal Smooth Muscles. *Adv Exp Med Biol* **1124**:3-46

Scallan JP, Davis MJ (2013) Genetic removal of basal nitric oxide enhances contractile activity in isolated murine collecting lymphatic vessels. *Journal of Physiology* **591**:2139-2156

Scallan JP, Wolpers JH, Davis MJ (2013) Constriction of isolated collecting lymphatic vessels in response to acute increases in downstream pressure. *J Physiol* **591**:443-459

Scallan JP, Wolpers JH, Muthuchamy M, Zawieja DC, Gashev AA, Davis MJ (2012) Independent and interactive effects of preload and afterload on the lymphatic pump. *Am J Physiol Heart Circ Physiol* **303**:H809-H824

Scallan JP, Zawieja SD, Castorena-Gonzalez JA, Davis MJ (2016) Lymphatic pumping: Mechanics, mechanisms and malfunction. *J Physiol* **594**:5749-5768

Schleifenbaum J, Kassmann M, Szijarto I, Hercule H, Tano JY, Weinert S, Heidenreich M, Pathan A, Anistan Y, Alenina N, *et al.* (2014) Stretch-Activation of Angiotensin II Type 1a Receptors Contributes to the Myogenic Response of Mouse Mesenteric and Renal Arteries. *Circ Res* **115**:263-272

Schulz ME, Akerstrom VL, Song K, Broyhill SE, Li M, Lambert MD, Goldberg TB, Kataru RP, Shin J, Braun SE, *et al.* (2025) Regulation of Collecting Lymphatic Vessel Contractile Function by TRPV4 Channels. *Arterioscler Thromb Vasc Biol*

Sharif-Naeini R, Folgering JH, Bichet D, Duprat F, Lauritzen I, Arhatte M, Jodar M, Dedman A, Chatelain FC, Schulte U, *et al.* (2009) Polycystin-1 and -2 dosage regulates pressure sensing. *Cell* **139**:587-596

Soni H, Peixoto-Neves D, Matthews AT, Adebiyi A (2017) TRPV4 channels contribute to renal myogenic autoregulation in neonatal pigs. *Am J Physiol Renal Physiol* **313**:F1136-F1148

Storch U, Blodow S, Gudermann T, Mederos YSM (2015) Cysteinyl leukotriene 1 receptors as novel mechanosensors mediating myogenic tone together with angiotensin II type 1 receptors-brief report. *Arterioscler Thromb Vasc Biol* **35**:121-126

Storch U, Mederos y Schnitzler M, Gudermann T. (2012) G protein-mediated stretch reception. *Am J Physiol Heart Circ Physiol* **302**:H1241-1249

Swain SM, Liddle RA (2021) Piezo1 acts upstream of TRPV4 to induce pathological changes in endothelial cells due to shear stress. *J Biol Chem* **296**:100171

To KHT, Gui P, Li M, Zawieja SD, Castorena-Gonzalez JA, Davis MJ (2020) T-type, but not L-type, voltage-gated calcium channels are dispensable for lymphatic pacemaking and spontaneous contractions. *Sci Rep* **10**:70

van Helden DF. (1993) Pacemaker potentials in lymphatic smooth muscle of the guinea-pig mesentery. *Journal of Physiology* **471**:465-479

Vinogradova TM, Maltsev VA, Bogdanov KY, Lyashkov AE, Lakatta EG (2005) Rhythmic Ca2+ oscillations drive sinoatrial nodal cell pacemaker function to make the heart tick. *Ann N Y Acad Sci* **1047**:138-156

Vinogradova TM, Zhou YY, Maltsev V, Lyashkov A, Stern M, Lakatta EG (2004) Rhythmic ryanodine receptor Ca2+ releases during diastolic depolarization of sinoatrial pacemaker cells do not require membrane depolarization. *Circ Res* **94**:802-809

von der Weid PY, Lee S, Imtiaz MS, Zawieja DC, Davis MJ. (2014) Electrophysiological properties of rat mesenteric lymphatic vessels and their regulation by stretch. *Lymphat Res Biol* **12**:66-75

Warthi G, Faulkner JL, Doja J, Ghanam AR, Gao P, Yang AC, Slivano OJ, Barris CT, Kress TC, Zawieja SD, *et al.* (2022) Generation and Comparative Analysis of an Itga8-CreER (T2) Mouse with Preferential Activity in Vascular Smooth Muscle Cells. *Nat Cardiovasc Res* **1**:1084-1100

Welsh DG, Morielli AD, Nelson MT, Brayden JE (2002) Transient receptor potential channels regulate myogenic tone of resistance arteries. *Circulation Research* **90**:248-250

Woo SH, Lukacs V, de Nooij JC, Zaytseva D, Criddle CR, Francisco A, Jessell TM, Wilkinson KA, Patapoutian A. (2015) Piezo2 is the principal mechanotransduction channel for proprioception. *Nat Neurosci* **18**:1756-1762

Woo SH, Ranade S, Weyer AD, Dubin AE, Baba Y, Qiu Z, Petrus M, Miyamoto T, Reddy K, Lumpkin EA, *et al.* (2014) Piezo2 is required for Merkel-cell mechanotransduction. *Nature* **509**:622-626

Wu G, D'Agati V, Cai Y, Markowitz G, Park JH, Reynolds DM, Maeda Y, Le TC, Hou H, Kucherlapati R, *et al.* (1998) Somatic inactivation of Pkd2 results in polycystic kidney disease. *Cell* **93**:177-188

Yamasaki E, Thakore P, Krishnan V, Earley S (2020) Differential expression of angiotensin II type 1 receptor subtypes within the cerebral microvasculature. *Am J Physiol Heart Circ Physiol* **318**:H461-H469

Yeung SY, Greenwood IA (2005) Electrophysiological and functional effects of the KCNQ channel blocker XE991 on murine portal vein smooth muscle cells. *Br J Pharmacol* **146**:585-595

Young MD, Behjati S (2020) SoupX removes ambient RNA contamination from droplet-based single-cell RNA sequencing data. *Gigascience* **9**

Zawieja SD, Castorena-Gonzalez JA, Scallan JP, Davis MJ (2018a) Differences in L-type Ca(2+) channel activity partially underlie the regional dichotomy in pumping behavior by murine peripheral and visceral lymphatic vessels. *Am J Physiol Heart Circ Physiol* **314**:H991-H1010

Zawieja SD, Castorena-Gonzalez JA, To KH, Gui P, Domeier TL, Davis MJ. (2018b) Electrical pacemaking in lymphatic vessels. In: Trebak M, Earley S (Eds). *Signal Transduction and Smooth Muscle* Boca Raton: CRC Press. pp. 324-359

Zawieja SD, Castorena JA, Gui P, Li M, Bulley SA, Jaggar JH, Rock JR, Davis MJ (2019) Ano1 mediates pressure-sensitive contraction frequency changes in mouse lymphatic collecting vessels. *Journal of General Physiology* **151**:532-554

Zawieja SD, Pea GA, Broyhill SE, Patro A, Bromert KH, Li M, Norton CE, Castorena-Gonzalez JA, Hancock EJ, Bertram CD, *et al.* (2023) IP3R1 underlies diastolic ANO1 activation and pressure-dependent chronotropy in lymphatic collecting vessels. *J Gen Physiol* **155**:e202313358

Zawieja SD, Pea GA, Broyhill SE, Patro A, Bromert KH, Norton CE, Kim HJ, Sivasankaran SK, Li M, Castorena-Gonzalez JA, *et al.* (2025) Cellular characterization of the mouse collecting lymphatic vessels reveals that lymphatic muscle cells are the innate pacemaker cells. *eLife* **12**

Zhong XZ, Harhun MI, Olesen SP, Ohya S, Moffatt JD, Cole WC, Greenwood IA (2010) Participation of KCNQ (Kv7) potassium channels in myogenic control of cerebral arterial diameter. *J Physiol* **588**:3277-3293

Zou W, Fan Y, Liu J, Cheng H, Hong H, Al-Sheikh U, Li S, Zhu L, Li R, He L, *et al.* (2025) Anoctamin-1 is a core component of a mechanosensory anion channel complex in C. elegans. *Nat Commun* **16**:1680

Zou Y, Akazawa H, Qin Y, Sano M, Takano H, Minamino T, Makita N, Iwanaga K, Zhu W, Kudoh S, *et al.* (2004) Mechanical stress activates angiotensin II type 1 receptor without the involvement of angiotensin II. *Nature Cell Biology* **6**:499-506

Zawieja SDPea GABroyhill SEPatro ABromert KHNorton CEKim HJSivasankaran SKLi MCastorena-Gonzalez JADrumm BTDavis MJ (2024) Characterization of the cellular components of mouse collecting lymphatic vessels reveals that lymphatic muscle cells are the innate pacemaker cells regulating lymphatic contractions. NCBI Gene Expression Omnibus. ID GSE277843 https://www.ncbi.nlm.nih.gov/geo/query/acc.cgi?acc=GSE277843

Peer reviews

Reviewer #1 (Public review):

Summary:

Davis and co-authors used many mouse models to investigate mechanisms that regulate the contractility of mouse popliteal collecting vessels, primarily chronotropy. Many of the mechanisms studied were previously shown to regulate pressure-induced constriction in small arteries. The authors use prior literature from the vasculature as a framework to test similar concepts in lymphatic vessels. The mouse models used provide evidence for and against the involvement of multiple proteins in regulating chronotropy and other contractile properties in lymphatic vessels. They propose that mechano-activation of GNAQ/GNA11-coupled GPCRs generates IP3, which induces Ca2+ release through IP3R1 and drives depolarization through the activation of ANO1 Cl- channels. Major concerns include the author's major conclusion that GNAQ/GNA11-coupled GPCRs contribute to chronotropy. This conclusion is not supported by the data presented.

Strengths:

One major strength of the study lies in the vast number of mouse knockout models that were used to test the importance of ion channels and G protein signaling pathways in the regulation of lymphatic vessel contractility. In this regard, the study is a valiant effort. The authors achieved several objectives to find that ANO1 and IP3R1 regulate chronotropy, and many other potential proteins do not regulate chronotropy. This study will have a major impact on the field if additional support for G proteins is provided.

Weaknesses:

Major conclusions concerning the involvement of G proteins are drawn from the global Gna11 knockout mouse models. This conclusion is weak. Global Gna11 knockout mice are highly likely to have a multifactorial phenotype that could create significant differences in the data. Control experiments need to be performed on vessels from the global knockout mice if these major conclusions are to be made. Similarly, pharmacological tools or alternative approaches to manipulate G proteins should be used to support the data from these mouse models to draw these major conclusions.

The Gnaq smKO mice are the most specific G protein model studied here. However, there is no phenotype. Do not discuss trends in the data. If the data are not significant, conclude so. If more experiments are required to reach significance, provide more data in the manuscript.

The conclusions repeatedly refer to a signaling pathway wherein the upstream component is GPCRs, which activate G proteins. While this may be the case, no GPCRs were identified here, and the involvement of G proteins is questionable, as the authors outline in lines 693-695 and noted above. The conclusions should be tempered, including in the abstract, unless additional experiments are performed to support the involvement of G proteins. Perhaps then the authors may be able to infer that GPCRs are involved.

Line 318. The point regarding the choice to use popliteal vessels versus IALVs will be unclear to the uninitiated, particularly as the authors previously used IALVs. Including additional

justification in the text and/or data from IALVs in Figure 1, which compares IALVs to popliteal vessels, would better explain the logic.

The conclusions drawn for TRPC6 and TRPC3 are less convincing. Germline global knockout mice, which are known to undergo compensation, were used, and high data variability is apparent. Using TRPC3 and TRPC6 blockers in the mouse models studied in Figure 4 would strengthen the arguments made regarding these proteins.

Did you perform power analysis to ensure that experimental numbers were sufficient to conclude that no statistical difference exists between datasets? If not, this needs to be done. For example, data shown in Figure 5C for tone and 6C for frequency and tone appear to be significantly different, but are concluded not to be so.

At the end of each result section, a concluding statement is made regarding the effects on pressure-induced chronotrophy. In many cases, there are additional effects of manipulating protein expression on other contractile properties. One example is for TRPC3 and TRPC6 (lines 414-416), but others are TRPV4, TRPV3, ENaC, Kir, Cav3.1/3.2, etc. Some interpretation is in the Discussion, but the concluding statements at the end of each result section should be expanded to summarize what the authors think the other significant differences in the data represent.

Kv7.4 channels. You state you have data (not shown) with linopiridine and XE991. Why not show those results here to support the experiments with the Kcnq4 smKO mice? Otherwise, I suggest you remove the statement from the unpublished data.

Figure 13A. Kcnj2 is modestly expressed in LECs, but very little is present in LMCs. This likely underlies the effect of barium. If you remove the endothelium, does the effect of barium disappear? While this is not the major focus of the study, the effects of barium are dramatic, and it should be made clear whether this is due to inhibition of Kir channels in smooth muscle or endothelial cells.

Figure 18C tone. Several values for losartan look different but are not labelled as such. Please clarify and discuss if different.

The manuscript should include raw data traces in figures that show the major pathways that you conclude regulate chronotropy.

https://doi.org/10.7554/eLife.109466.1.sa2

Reviewer #2 (Public review):

Summary:

In this study, Davis et al. embarked on the quest for the molecular elements responsible for the regulation of lymphatic phasic contractile activity in response to variation of transmural pressure, a mechanism (termed pressure-induced lymphatic chronotropy by the authors) critical for drainage of interstitial fluid from the tissue and transport of lymph back to the blood circulation. Their aim was to investigate the mechanism(s) involved in the pressure-induced regulation of lymphatic pumping, and test whether activation of cation channels, shown in other systems to play mechanosensitive roles are directly at play, and/or whether mechano-activation of GNAQ/GNA11-coupled GPCRs is necessary to generate second messengers to activate those channels, as it has been suggested for the regulation of myogenic tone in arteries. To achieve their goal, the authors used their well-described, highly reliable protocols of mouse lymphatic vessel isolation, pressure myography, and data acquisition to obtain frequency-pressure relationships and other contractile function parameters from transgenic mice where specific channels or molecular elements of interest have been ablated. They combined these data with scRNAseq analysis of these gene targets to

determine their respective role and levels of expression in lymphatic muscle cells. Their conclusion is that none of the exhaustive list of tested ion channels was critical, except ANO1 Cl channels, part of the contractile pacemaker mechanism, but that transmural pressure activates GNAQ/GNA11-coupled GPCRs, which generate IP3 to induce SR Ca2+ release through IP3R1 and activate ANO1-mediated depolarization.

Strengths:

The manuscript's strengths reside primarily in very robust, clean, and unequivocal pressure myography data and analysis. The research team is mastering these techniques they developed more than a decade ago and have implemented in mouse lymphatics to study their contractile properties, with consistent and convincing outcomes. They also provide data from an impressive list of transgenic mice in order to determine the role of the targeted gene in pressure-induced lymphatic chronotropy, relying on pharmacological small molecule inhibitors only when necessary. Finally, the use of scRNAseq analysis they gathered from previously published datasets brings novelty with respect to the expression of the genes of interest in all populations of cells comprising the lymphatic vessels, but more critically, to validate or contrast the potential impact of genetic alteration of the given gene on the ability of lymphatic muscles to respond to a change in pressure.

Weaknesses:

The main weakness may reside in the fact that while the authors provide a convincing demonstration that GNAQ/GNA11 are involved in the regulation of the F-P relationship, they give little evidence of the involvement of "upstream" receptors. Indeed, inhibition of AT1R, shown to be involved in myogenic regulation of arteries (a phenomenon the authors rightfully compare to pressure-induced lymphatic chronotropy), didn't lead toa similar effect (decrease in F-P) in lymphatic vessels. Arguably, other GPCRs might be involved in lymphatic vessels, but as such information is not provided in the manuscript, the author's conclusions should be dampened. More in-depth discussion would be required. In fact, it can be argued that the discussion is very restricted with respect to the amount of data and information the manuscript provides.

Overall, the authors convincingly achieved their aim by performing an impressive number of technically challenging experiments, leading to solid datasets. While these support their main conclusions, a more elaborate discussion might be required to refine them.

This study is likely to have an important impact on the field as it provides some answers to the lingering question of how lymphatic vessels regulate their contractile activity to variation in transmural pressure and certainly proposes an experimental means to further explore and address that question.

https://doi.org/10.7554/eLife.109466.1.sa1

Reviewer #3 (Public review):

In this manuscript, Davis and colleagues aimed to identify the molecular sensors and signaling cascade that enable collecting lymphatic vessels to increase their spontaneous contraction frequency in response to intraluminal pressure (pressure-induced chronotropy). They tested whether the process is similar to blood vessel myogenic constriction by relying on cation channels (TRPC6, TRPM4, PKD2, PIEZO1, etc.) or instead require the activation of G-protein-coupled receptors (presumably mechanosensitive GNAQ/GNA11-coupled receptors), using ex vivo pressure myography of mouse popliteal lymphatics, smooth muscle-specific conditional knockouts, quantitative PCR validation, and single-cell RNA sequencing for target prioritization. The authors convincingly demonstrate that pressure-induced chronotropy does not require the cation channels implicated in arterial myogenic tone but is blunted by

deletion of GNAQ/GNA11 or IP3 receptor 1, supporting a model of GPCR > IP3 > Ca2+ release > Cl^- channel activation > depolarization. The core conclusion is robust. The work redefines lymphatic pacemaking as G-protein-coupled receptor-dependent mechanotransduction, distinct from arterial mechanisms, and provides a genetically validated toolkit that is useful for studying lymphatic function and dysfunction.

Strengths:

(1) The data are of high quality and highly sensitive functional readouts

(2) The systematic genetic targeting is a major strength that overcomes pharmacological artifacts

(3) Careful quantitative analyses of frequency-pressure slopes

Weaknesses:

(1) The use of inguinal-axillary vessels for single-cell RNA sequencing rather than the popliteal segment studied functionally.

(2) No direct testing of the specific G-protein-coupled receptor involved.

https://doi.org/10.7554/eLife.109466.1.sa0

Author response:

We thank the reviewers and editors for their insightful comments on our manuscript. We intend to submit a revised manuscript that addresses all concerns raised by the reviewers. A major limitation identified by the reviewers was our inability to identify one or more specific mechanosensitive GPCRs in lymphatic muscle cells (LMCs). To address this concern, we plan to include several additional figures in the revised manuscript. One figure will list the 136 GPCRs identified in LMCs by our scRNAseq analysis, based on the list of validated GPCRs in *https://esbl.nhlbi.nih.gov/Databases/GPCRs/index.html* and olfactory GPCRs listed in *https://esbl.nhlbi.nih.gov/Databases/GPCRs/MouseHumanRatORs.html*. We plan to arrange the data in a hierarchical manner according to their expression level and denote their heterotrimeric GTP-binding protein alpha subunit(s), if known. To reinforce our finding that pressure-induced chronotropy in LMCs is mediated through Gq/11, we will present additional data testing the effects of acute Gq/11 inhibition with YM-254890 (a selective Gq/11 inhibitor) on the frequency-pressure relationship of popliteal vessels, as suggested by one reviewer. We will address concerns regarding the potential regional differences in lymphatic contractile regulation arising from our use of popliteal lymphatic vessels for contraction assays and expression analysis of LMCs obtained from Inguinal-Axillary lymphatic vessels (IALVs). To account for possible differences between the two, we will test pressure responses of IALVs from double Gq/11 knockout mice and test responses of wild-type IALVs to acute administration of YM-25489.

Our preliminary analysis of the 136 GPCRs in LMCs revealed a shorter list of 10 GPCRs that are expressed in at least 50% of LMCs (based on the IALV scRNAseq dataset). Since existing evidence from our studies, and those of other investigators, suggests that any LMC is capable of initiating pacemaking, we consider it reasonable to impose this requirement.

Gene	Description	Fraction of LMCs expressing
Adgre5	Adhesion G protein-coupled receptor, subfamily E	0.65
Adgrl1	Adhesion G protein-coupled receptor, subfamily L	0.68
Adgrl2	Adhesion G protein-coupled receptor, subfamily L	0.89
Ednra	Endothelin receptor	0.74
Fzd4	G protein-coupled receptor, Class F frizzled	0.68
Fzd8	G protein-coupled receptor, Class F frizzled	0.68
Npr3	Transmembrane guanylyl cyclase	0.57
Npy1r	Neuropeptide receptor	0.87
Tbxa2r	Prostaglandin receptor	0.51
Olfr1033	Olfactory receptor	0.63

Author response table 1.

We plan to use pharmacologic inhibitors to test as many of these candidates as possible. Unfortunately, inhibitors are not available for many of the GPCRs listed above, but we will test Npr3, Npy1R, and Ednra; a negative result for Tbxa2r has already been documented in a previous study (Schulz et al. ATVB 2025). Even if this strategy does not lead to identification of one or more specific GPCRs involved in LMC pressure transduction, it will narrow the list of possible candidates that need to be tested in future experiments.

https://doi.org/10.7554/eLife.109466.1.sa4